# **CEDAR 2015**

Walker-Ames Room, Kane Hall University of Washington



Seattle, Washington

**MLT Poster Session** 

Tuesday June 23, 2015

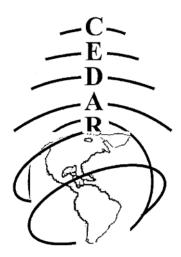


### **Table of Contents**

### **Coupling of the Upper Atmos with Lower Alts**

COUP-01	Richard Eastes, Global-scale Observations of the Limb and Disk (GOLD) Mission – Observing Forcing of the Thermosphere-Ionosphere System from Above and Below
COUP-02	Federico Gasperini, Wave Coupling between the Lower and MiddleThermosphere as viewed from TIMED and GOCE
COUP-03	Rosmarie J. de Wit, Quantifying the influence of the stratosphere on the mesosphere and lower thermosphere
COUP-04	Matthew Grawe, Prediction and Analysis of Tsunami-Ionospheric Coupling Efficiency at Large Spatial Scales
COUP-05	Cissi Lin, Implementation of Spectral Gravity Wavefield to the Global Ionosphere Thermosphere Model (GITM)
COUP-07	Joe McInerney, WACCM-X: Recent Improvements, Current Development, and Future Plans
COUP-08	Justin Mabie, Observation of rocket induced acoustic waves in the Ionosphere4
COUP-09	Marcin Pilinski, Seasonal Variability in Global Eddy Diffusion and the Effect on Thermospheric Neutral Density4
COUP-10	Jack Chieh Wang, Tidal Variability Due to the Quasi-biennial Oscillation and Ionospheric Responses

### Instr or Techniques for Middle Atmosphere Obs

ITMA-01	Stephen Andrew, Hall Multi-Beam, High-Power Rayleigh Lidar for Study of the Dynamics of the Middle and Upper Atmosphere	
ITMA-02	Marcos Jose Inonan, Measuring Ion Spectra in the D-region using Arecibo Incoherent Scatter Radar	5

ITMA-03	Jintai Li, Mesospheric turbulence detection and characterization with AMISR- class radars: Retrieval method and case studies using PFISR
ITMA-04	Eliana Nossa, ISR Wind Measurements for the Mesosphere and Lower Thermosphere Region - New Techniques and Observations
ITMA-05	Peter Panka, Study of vibrational-vibrational (V-V) energy exchange between CO2 isotopes in the middle and upper atmospheres of Earth and Mars
ITMA-06	Cody Vaudrin, Multistatic Meteor Wind Radar and Results from a Recent Observation Campaign of the Geminids Meteor Shower in Adelaide, Australia7
ITMA-07	Stuart Johnson, Low-cost Airglow Imager: Integrating CEDAR Science Into the Undergraduate Research and Course Curriculum7

### Data Management

DATM-01	Luis Navarro Dominguez, Online Monitoring System for Lidar Operations and	
	Data Handling at ALO-USU	3

### Long Term Variations of the Mesosphere and Lower Thermosphere

### Meteor Science other than wind observations

METR-02	Boyi Gao, High-Altitude Radar Meteors Observed at Jicamarca Radio Observatory using Multi-Baseline Interferometric Technique
METR-03	Robert Anthony Haaser, Understanding the atmospheric and Ionospheric response to hypersonic objects in the Earth's atmosphere9
METR-04	Ashish Goel, Measurements of Hypervelocity Impact Plasma Using a Plasma Spectrometer
METR-05	Yayu Monica Hew, Time-resolved Emission Characteristics of Hypervelocity Impact Generated Flash
METR-06	Daniel Kellett, Accurate Detection of Micro-Meteor Observations by the Arecibo 430 MHz Incoherent Scatter Radar11
METR-07	Lorenzo Limonta, Multi-instrument detection of meteoroids and ablation characterization
METR-08	Liane Kathryn Tarnecki, Spectra of Full 3-D PIC Simulation of Evolving Meteor Trails
METR-09	Qian Zhu, High spatial and temporal resolution radar measurements of meteor fragmentation at the Jicamarca Radio Observatory
METR-10	Ana Maria Tarano, Characterization of Non-Specular Meteors Detected by a Non-Equatorial Radar
METR-11	Alex Fletcher, Weibel instability in meteoroid impact-produced plasmas13
METR-12	Benjamin Thomas Spangler, A Comparison of Optical and Radar Meteoroid Mass Estimates Using Simultaneous Observations

### MLT Gravity Waves

MLTG-01	Erin H Lay, Ionospheric acoustic and gravity waves associated with mid-latitude
	thunderstorms
MLTG-02	Ryan Matthew Agner, Local Gravity Wave Effects on the DW1 Tidal Variability In WACCM/eCMAM

MLTG-03	Christopher Heale, The relative importance of temperature and wind medium scale wave perturbation fields in refracting small-scale gravity waves
MLTG-04	Bing Cao, Observational and Modeling Study of Gravity Wave Propagation Through Reflection and Critical Layers15
MLTG-05	Yun Zhang, The study of gravity wave components with different vertical scales in the stratosphere based on SABER temperature data
MLTG-06	Hosik Kam, Observation of mesospheric gravity waves with an All-Sky Camera in King Sejong Station, Antarctica (62° 13'S, 58° 47'W)15
MLTG-07	Dhvanit Mehta, Gravity Wave Sources over South Pole16
MLTG-08	Michael R. Negale, Investigating Thermospheric Gravity Wave Amplitudes in the High Arctic
MLTG-09	Jonathan Pugmire, Satellite measurements of mesospheric gravity wave temperature variances over the Andes
MLTG-10	Ahmad Talaei, Horizontal phase speed distribution of gravity waves observed in mesospheric temperature maps
MLTG-11	Colin Charles Triplett, Gravity wave activity over Chatanika, Alaska and its relationship to the wind field and geostrophic adjustment
MLTG-12	Chris William Vail, Gravity Wave Parameter Distribution over multiple seasons using an All Sky Imager in Eureka, Nunavut, Canada
MLTG-13	Haoyu Li, Statistical Study of High to Medium Frequency Mesoscale Gravity Waves over the Central US using Temperature Mapper, CRRL Na Lidars, and ECMWF
MLTG-14	Johnathon S. Gay, Undergraduate High Impact Learning Through Ray Tracing of Atmospheric Gravity Waves
MLTG-15	Luis Navarro Dominguez, Detection and estimation of Gravity Wave parameters from the Jicamarca All-Sky Imager

### MLT Lidar Studies

MLTL-01	Vincent B. Wickwar, The transition from summer-to-winter temperatures between 70 and ~115 km as observed with the ALO-USU Rayleigh lidar20
MLTL-02	Ian Barry, Stratospheric and MLT Temperature and Horizontal Wind Vector Collection Using Na-DEMOF Receivers
MLTL-03	Katrina Bossert, Instabilities, Critical Layers, and Secondary Gravity Wave Generation in the Mesosphere and Lower Thermosphere During the DEEPWAVE Campaign
MLTL-04	Cao Chen, A statistical study of the 4-9 h waves in the Antarctic middle and upper atmosphere observed by lidar
MLTL-05	Yafang Guo, Sodium observation in the lower thermosphere (120-160 km) at the Andes Lidar Observatory
MLTL-06	Leda Sox, Changing Atmospheric Composition and the Retrieval of Rayleigh Lidar Temperatures in the Lower Thermosphere
MLTL-07	Wentao Huang, Design and implement a new Na Faraday filter for STAR Na Doppler lidar at Boulder to make high-quality daytime measurements

### Mesosphere or Lower Thermosphere General Studies

MLTS-01	Erin Dawkins, CO2 in the MLT: constraining the CO2(v2)-O quenching rate coefficient
MLTS-02	Xuguang Cai, Investigation on how the strong Sporadic Na layer formed by model simulation
MLTS-03	Takanori Nishiyama, Height and time characteristics of seasonal and diurnal variations in PMWE based on 1 year observations by the PANSY radar (69.0°S, 39.6°E)
MLTS-04	Yi Chung Chiu, The Equatorial OH Airglow Analysis by ISUAL Instrument on Board the FORMOSAT 2 Satellite
MLTS-05	Neal R. Criddle, Coordinated temperature measurements in Logan, UT, USA24

MLTS-06	Cornelius Csar Jude Salinas, Seasonal Variations of TIMED/SABER Carbon Dioxide based Eddy Diffusion Coefficients in the MLT Region	24
MLTS-07	Julio Alberto Oscanoa, Mesospheric winds estimation algorithms for Jicamarca All-Sky Meteor radars	

### MLT Other Tidal, PWs, or SSWs

MLTT-01	Quan Gan, Observations of thermosphere and ionosphere changes due to the dissipative 6.5-day wave in the lower thermosphere
MLTT-02	Weichun Fong, First climatology of temperature structure from 0 to 110 km during 2011-2014 and mechanism study of winter temperature tides of fast amplitude growth above 100 km at McMurdo (77.8S, 166.7E), Antarctica25
MLTT-03	Loren Chang, Seasonal and quasi-biennial variations in ionospheric tidal signatures using HHT analysis
MLTT-04	Jia-Ting Lin, A Study of thermospheric-ionospheric response to the 2009 stratospheric sudden warming by using an assimilative TIME-GCM with SAMI3 model simulations
MLTT-05	Xian Lu Lidar, and satellite studies of the vertical coupling of eastward propagating planetary waves with periods of 1–5 days from the stratosphere to the lower thermosphere in the winter Antarctic
MLTT-06	Garima Malhotra, Interhemispheric Comparison of Seasonal Mesospheric Tidal Activity observed by mid-latitude SuperDARN Radars27
MLTT-07	You Yu, Seasonal variations of MLT tides revealed by a meteor radar chain based on HMD analysis
MLTT-08	Vu Nguyen, Observations of Secondary Waves Arising from QTDW-DW1 Interaction
MLTT-09	Mary Beth Bradley, Stationary planetary waves and their momentum budgets in eCMAM30
MLTT-10	Nirmal Nischal, Photochemical modeling of nonmigrating tides in the 15 µm infrared cooling of the lower thermosphere and comparison with SABER

MLTT-11	Ashan Vitharana, Statistical characteristics of short-term variability of diurnal tides in eCMAM30	.29
MLTT-12	David Warder, Seasonal variations of Hough modes in DW1 and DS0	.30
MLTT-13	Shengyang Gu, Influence of the sudden stratosphere warming on quasi-2 day waves	.30
MLTT-14	Austin Gornet, Examination of sudden stratospheric warming effects of non- migrating diurnal tides	.30
MLTT-15	Brittany A. Marriott, Neutral Temperature and Horizontal Wind in the Thermosphere	.31

### <u>Sprites</u>

SPRT-01	Levi Boggs, Analysis of two thunderstorms producing three negative sprites on 12 September 2014
SPRT-02	Mohammad Ahmad Salem, Effects of Thunderstorm Electrostatic Fields on the Conductivity of the Lower Ionosphere
SPRT-03	Salih Mehmed, Bostan Preliminary Results of a Software Defined Radar System to Detect Sprites

### **Stratosphere Studies and Below**

STRA-01	David K. Moser, Comparing USU Rayleigh Lidar and Assimilative Model	
	Temperatures at 45 km	32

### **CEDAR Workshop – MLT Poster Session Abstracts**

Day 1 – Tuesday, Jun 23, 2015

### **Coupling of the Upper Atmos with Lower Alts**

### COUP-01 Global-scale Observations of the Limb and Disk (GOLD) Mission – Observing Forcing of the Thermosphere-Ionosphere System from Above and Below by Richard Eastes

Status of First Author: Non-student, PhD

Authors: Richard Eastes, William McClintock, Alan Burns, D. N. Anderson, L. Andersson, M. Codrescu, R. E. Daniell, S. England, S. Evans, J. Harvey, A. Krymonos, M. Lankton, J. D. Lumpe, A. D. Richmond, D. W. Rusch, O. Siegmund, S. C. Solomon, D. J. Strickland, T. N. Woods, R. S. Lieberman, C. R. Martinis, J. Oberheide, S. A. Budzien, K. Dymond, F. G. Eparvier, H. Foroosh, and A. Aksnes

**Abstract**: The GOLD mission will provide unprecedented imaging of the Earth's space environment and its response to forcing from the Sun and the lower atmosphere. The mission will fly a far ultraviolet imaging spectrograph and is scheduled for launch into geostationary (GEO) orbit in October 2017 as a hosted payload on a commercial communications satellite flying over eastern South America. From this vantage point GOLD will repeatedly image the American hemisphere at a thirty-minute cadence, providing an excellent opportunity for collaborative studies with the existing ground-based network in South America. Fundamental parameters that will be derived from these measurements include composition (O/N2) and temperature of the neutral atmosphere on the dayside disk. Imaging of atmospheric composition, at only a daily cadence, has already provided many new insights into the behavior of the Thermosphere-Ionosphere (T-I) system. Combining composition with simultaneous temperature images will provide revolutionary insights into the behavior of the T-I system and its response to external forcing. Since GOLD will repeatedly observe the same geographic locations, it can distinguish between spatial and temporal variations in the TI system caused by geomagnetic storms, variations in solar EUV, and forcing from the lower atmosphere. GOLD's measurements and observing approach will give the scientific community a new understanding of the T-I system.

# COUP-02 Wave Coupling between the Lower and Middle Thermosphere as viewed from TIMED and GOCE - by Federico Gasperini

Status of First Author: Student IN poster competition, PhD

Authors: Federico Gasperini, Jeffrey Forbes, Eelco Doornboos, and Sean Bruinsma

**Abstract**: Vertical coupling between the lower and middle thermosphere due to the eastward propagating diurnal tide with zonal wavenumber 3 (DE3) and the 3.5-day Ultra-Fast Kelvin Wave (UFKW) is investigated using TIMED-SABER temperatures near 100 km and GOCE neutral densities and zonal winds near 260 km. The analysis is performed between +/- 45 deg. latitude during 2011, when reliable and continuous measurements are available.

With geomagnetic and solar effects removed, DE3 and the UFKW are identified as dominant sources of day-to-day variability at both heights. Evidence is found for the vertical propagation of DE3 and the UFKW from the lower to middle thermosphere over a range of time scales. Over 60\% of the variance due to DE3 and the UFKW at 260 km is traceable to variability occurring at 100 km. The not exact agreement is thought to be due to the influences of wave-wave interactions, zonal mean winds, dissipation, and inherent transience that interfere with one-to-one mapping of structures between 100 and 260 km.

Spectral and temporal analyses of the SABER and GOCE data also reveal the presence of sidebands due to the modulation of DE3 by the UFKW. These secondary waves are responsible for up to 10% to 20% of the longitudinal and day-to-day variability. Overall, vertical propagating waves together with sidebands from DE3-UFKW nonlinear interactions are responsible for 60% to 80% of the total variability, while geomagnetic and solar effects correlated with ap and F10.7 account for less than 20% of the variance.

### **COUP-03** Quantifying the influence of the stratosphere on the mesosphere and lower thermosphere - by Rosmarie J. de Wit

Status of First Author: Non-student, PhD

Authors: R.J. de Wit, R.E. Hibbins, P.J. Espy, D. Janches, D.C. Fritts

**Abstract**: Selective filtering of upward propagating gravity waves (GWs) in the stratospheric wind field plays an important role in determining which part of the GW spectrum reaches the mesosphere and lower thermosphere (MLT). As GWs are believed to be the main driver of the MLT general circulation, it is clear that the stratosphere is key in coupling the MLT to the lower atmosphere. However, observations quantifying the influence of the stratosphere on the MLT are lacking. In this study, the GW spectrum reaching the MLT is quantified by new generation meteor radar observations of GW momentum flux and forcing. The wind field is derived by combining MERRA reanalysis and meteor radar winds. To study the relation between MLT GW forcing and selective filtering of upward propagating GWs by the zonal wind field in the stratosphere, an estimate of the zonal wind experienced by a symmetric distribution of upward propagating GWs is introduced. The 'net zonal wind', defined as the average of the most eastward and most westward wind within the column below the MLT, is subsequently related to the GW forcing to derive a quantitative relationship between the stratosphere and the MLT. This relationship is tested for a wide range of dynamical conditions.

### COUP-04 Prediction and Analysis of Tsunami-Ionospheric Coupling Efficiency at Large Spatial Scales - by Matthew Grawe

Status of First Author: Student IN poster competition, Undergraduate

Authors: Matthew Grawe and Jonathan Makela

**Abstract**: Comparisons between the ionospheric signatures of the 11 March 2011 Tohoku and 28 October 2012 Haida Gwaii tsunamis show a dependence on observation geometry and the orientation of the tsunami relative to the geomagnetic field. These anisotropies, present in the TEC signal and airglow measurement, reveal that certain tsunami arrival directions are easier to observe than others. Additionally, the enhancement of the perturbation depends on the interplay between the receiver-satellite line-of-sight (LOS) and the phase fronts of the internal gravity wave. Here, we explore the effects of tsunami properties (such as wavelength, period, speed, and direction) on coupling efficiency. We also present a method for quickly predicting the coupling efficiency at a specific location in the ocean that is free of computationally expensive simulation. The prediction method is used to analyze the observability of several historical tsunamis.

### COUP-05 Implementation of Spectral Gravity Wavefield to the Global Ionosphere Thermosphere Model (GITM) - by Cissi Lin

Status of First Author: Non-student, PhD

Authors: Cissi Lin, Yue Deng, Cheng Sheng, Douglas Drob

**Abstract**: Waves of various spatial and temporal scales, including acoustic waves, gravity waves, tides, and planetary waves, modify the dynamics of the terrestrial atmosphere at all altitudes. Perturbations caused by the natural and mankind activities on the ground, such as volcano eruptions, earthquakes,

explosions, propagate upward and impact the upper atmosphere. Among these waves, propagation of the atmospheric acoustic waves is particularly sensitive to the fine structure of the background atmosphere. However, the sub-grid gravity waves are currently poorly measured especially at the altitudes above 100 km and is computationally too expensive for most of the models to incorporate properly. Since GITM allows for non-hydrostatic solutions and has a flexible resolution, it is ideal for the study of vertical propagating waves. In this study, a time-varying spectral gravity wavefield propagated from the ground is implemented into GITM to capture the statistically averaged sub-grid background structure that is crucial to the upper atmospheric models. The influence of the vertical wavelength of the sub-grid gravity waves at ~100 km can be as short as 1 km, the vertical resolution of the model should play an important role to the simulation of the vertical wave propagation. To illustrate this importance, GITM has been run with vertical resolution of both 0.15 and 0.30 of the scale height. The gravity wave propagation from the two runs has been compared.

### COUP-06 Magnetospheric Coupling to the Global Electric Circuit - by Greg Lucas

Status of First Author: Student IN poster competition, Masters

#### Authors: Greg Lucas and Jeff Thayer

Abstract: The Earth's Global Electric Circuit (GEC) embodies the electrical pathways by which currents flow from electrified tropospheric clouds to the ionosphere and close through return currents from the ionosphere to the Earth's surface, with the intervening atmosphere determining the resistance of the circuit. To investigate geophysical influences on this pathway, a GEC model has been developed within the Whole Atmosphere Community Climate Model (WACCM) framework to solve for conductivities, currents and electric fields within the atmosphere. The GEC community has made significant advances in understanding the driving forces within the atmosphere, focusing on the global thunderstorm and conductivity distribution. However, the ionosphere and ground are considered to be held at constant potentials which is a good assumption at low-latitudes but not a valid assumption at high latitudes. This new GEC model introduces a pathway by which the magnetospheric current systems can influence the currents within the GEC. This coupling is achieved by modifying the ionospheric potential through the imposed potentials introduced by the magentospheric current system. This effect is represented in the GEC/WACCM framework by employing the Weimer potential model at high-latitudes and combining it with the GEC potential. A unique coupling signature at high-latitudes in the GEC is observed due to the diurnal rotation of high-latitude potentials (geomagnetically controlled) with lightning-induced potentials (geographically controlled). Typical diurnal variations and their magnitudes during solar quiet periods will be demonstrated and compared to observational data in the Antarctic region. Finally, to demonstrate shorter time-scale features the impact of severe solar storms on the GEC currents and electric fields measured on the ground will be presented.

### COUP-07 WACCM-X: Recent Improvements, Current Development, and Future Plans by Joe McInerney

Status of First Author: Non-student, Masters

Authors: Joe McInerney, Ben Foster, Hanli Liu, Stan Solomon, Chris Fischer, Liying Qian, Wenbin Wang, Art Richmond, Gang Lu, Astrid Maute, Mike Wiltberger

**Abstract**: With the advent of faster supercomputers with increasing numbers of processors, producing accurate climate simulations with numerical models, which cover the entire Earth's atmosphere from the ground to the bottom of the exosphere, is becoming more realistic. One such model is the Whole Atmosphere Community Climate Model - eXtended (WACCM-X) currently under development in the High Altitude Observatory (HAO) at the National Center for Atmospheric Research in Boulder, Colorado. An atmospheric component option of the Community Earth System Model (CESM), WACCM-X is based on other CESM options, the Community Atmosphere Model (CAM) and the Whole Atmosphere

Community Climate Model (WACCM). While CAM extends from the ground to ~30km and WACCM to ~140km, WACCM-X has a model top of ~500km. Here we present some background on the previous CESM release version of WACCM-X, discuss some recent enhancements to be included in the next WACCM-X release, and look forward at the future of the model.

#### COUP-08 Observation of rocket induced acoustic waves in the Ionosphere - by Justin Mabie

Status of First Author: Student NOT in poster competition, Masters

Authors: Justin Mabie and Terrence Bullett

**Abstract**: Ionospheric disturbances after rocket launches were observed with the Vertically Incident Pulsed Ionospheric Radar (VIPIR). These disturbances are attributed to vertically propagating infrasonic acoustic waves. Measurements are taken with high temporal resolution at multiple altitudes and results of the analysis are presented.

# COUP-09 Seasonal Variability in Global Eddy Diffusion and the Effect on Thermospheric Neutral Density - by Marcin Pilinski

Status of First Author: Non-student, PhD

Authors: Marcin Pilinski, Geoff Crowley, Jon Wolfe

**Abstract**: We describe a method for making estimates of the seasonal variability in global-average eddy diffusion coefficients based on measurements of satellite drag. Eddy diffusion values as a function of time between January 2004 and January 2008 were estimated from residuals of neutral density measurements made by the CHallenging Minisatellite Payload (CHAMP) and simulations made using the Thermosphere Ionosphere Mesosphere Electrodynamics - Global Circulation Model (TIME-GCM).

The eddy diffusion coefficient results are quantitatively consistent with previous estimates based on satellite drag observations and are qualitatively consistent with other measurement methods such as sodium LIDAR observations and eddy-diffusivity models. The eddy diffusion coefficient values estimated between January 2004 and January 2008 were then used to generate new TIME-GCM runs. Based on these results, the RMS difference between the TIME-GCM model and density data from a variety of satellites is reduced by an average of 5%.

The feasibility of estimating a latitude-dependent eddy-diffusion coefficient is also investigated. For this part of the poster, data from both CHAMP accelerometers as well as from the aerodynamic-drag analysis of orbiting spheres is analyzed. Although the use of global values improves modeled neutral densities, there are some limitations of this method, which are discussed. These include the aliasing of geomagnetic and solar forcing into the estimate of eddy diffusion. Overall, our results indicate that global thermospheric density modeling can be improved by using data from a single satellite like CHAMP. This approach also demonstrates how eddy diffusion could be estimated in near real-time from satellite observations and used to drive a global circulation model like TIME-GCM.

### COUP-10 Tidal Variability Due to the Quasi-biennial Oscillation and Ionospheric Responses - by Jack Chieh Wang

Status of First Author: Student IN poster competition, Masters

Authors: Jack C. Wang, Loren C. Chang, Qian Wu

**Abstract**: The Quasi-biennial Oscillation (QBO) is a persistent oscillation in the zonal mean zonal winds of the low latitude middle atmosphere that is driven by breaking planetary and gravity waves, with a period near two years. The atmospheric tides that dominate the dynamics of the mesosphere and lower

thermosphere region (MLT, between heights of 70 to 120 km) are excited in the troposphere and stratosphere, and propagate through QBO-modulated zonal mean zonal wind fields. This allows the MLT tidal response to also be modulated by the QBO, with implications for ionospheric/thermospheric variability. In this research, we develop an empirical model to isolate QBO-related tidal variability in the MLT diurnal and semidiurnal tides using values from assimilated TIMED satellite data. Tidal fields corresponding to QBO eastward and westward phases are then used to drive the NCAR Thermosphere-Ionosphere-Electrodynamics General Circulation Model (TIE-GCM), and differences in major ionospheric / thermospheric features examined.

### **Instruments or Techniques for Middle Atmosphere Observations**

## ITMA-01 Multi-Beam, High-Power Rayleigh Lidar for Study of the Dynamics of the Middle and Upper Atmosphere - by Stephen Andrew Hall

Status of First Author: Student IN poster competition, PhD

#### Authors: Stephen Hall and Gary Swenson

**Abstract**: While single-beam Rayleigh lidar have been in common usage for decades, their lack of horizontal resolution limits their ability to study the dynamic structure of the atmosphere. An experimental multi-beam lidar transmitter is under development at the University of Illinois that overcomes this problem by the simultaneous generation of a fan of closely-spaced near-vertical beams from a single high-power pulsed laser, allowing for the resolution of horizontal features on the order of tens of meters and capturing of dynamic events such as billows and overturnings. This transmitter is coupled with a digital receiver with a variable readout frequency that allows for quickly variable vertical resolution that can be optimized for the size of various features. Simulations of the current configuration of the lidar suggest useful measurements of the neutral atmosphere up to 120 km, but this limit is a function not only of signal and noise but also of the pulse repetition rate of the laser and the number of beams generated. This provides the lidar the ability to be reconfigured for even higher altitudes when coupled with a large telescope such as the 8-meter mirror on Cerro Pachon in Chile. Future iterations of this lidar would allow for the number of beams and the horizontal and vertical resolutions to be varied without any changes in the hardware, permitting quick transitions between configurations optimized for various dynamic atmospheric features.

### ITMA-02 Measuring Ion Spectra in the D-region using Arecibo Incoherent Scatter Radar by Marcos Jose Inonan

Status of First Author: Student IN poster competition, Undergraduate

### Authors: John D. Sahr and Marcos J. Inonan

**Abstract**: An incoherent scatter experiment using high range resolution has been implemented at Arecibo. This experiment was intended to facilitate the measurement of Ion and Plasma spectra in the D region where collisions frequency between electrons and ions are almost imperceptible. By taking advantage of the signal correlation times at the D region are relatively long compared to the sampling interval, coherent integration in range has been used in order to increase the signal to noise ratio (SNR). Additionally, pulse to pulse incoherent integration (mean and median filter) have been also applied in order to improve the fitting quality.

The ion component of the ISR spectrum has been fitted to three known functions: the (Folded) Lorentizan, Gaussian and Voigt profile. Each model is parametrized by the estimation of power spectra, altitude variation of full width at half maximum (FWHM), Doppler velocity and Noise Level. Each parameteralong with its interquartile range- will be compared for each model fitted. While the uncoded long pulse used in this experiment provided ample sensitivity for ion measurement, ground clutter frequently impacts the analysis. The much wider bandwidth of the electron spectrum makes it difficult to recover in this data set.

### ITMA-03 Mesospheric turbulence detection and characterization with AMISR-class radars: Retrieval method and case studies using PFISR - by Jintai Li

Status of First Author: Student IN poster competition, Masters

Authors: Jintai Li, Richard L. Collins, David E. Newman and Michael J. Nicolls

**Abstract**: A recent study has shown the ability to detect turbulence in the mesosphere (D-Region) using the Advanced Modular Incoherent Scatter Radar (AMISR) at Poker Flat Research Range (PFISR, Nicolls et al, 2011). AMISR-class radars have narrow beam and high vertical resolution. We review the principles and practices of incoherent scatter radar with a focus on detection of D-region turbulence using radar spectra. We review the geometry of the turbulence and the radar, comparing the turbulent, plasma, and radar spatial scales. We present a turbulence retrieval algorithm using a Voigt function spectral line. The Voigt function, as in optics, represents as primary Lorentzian line (the ion-line subject to collisions) convolved with a Gaussian line (Doppler broadening by turbulence). We present initial case studies to illustrate our technique, using the spectra of the vertical beam of PFISR to detect and characterize mesospheric turbulence. For the vertical beam we can neglect broadening processes due to beam and shear broadening by the winds. We use the root mean square velocity derived from the Gaussian component of the Voigt spectra to calculate the turbulent energy dissipation rate. We discuss how combined radar and lidar measurements can be used to study turbulence in the presence of Mesospheric Inversion Layers (MILs).

### ITMA-04 ISR Wind Measurements for the Mesosphere and Lower Thermosphere Region -New Techniques and Observations - by Eliana Nossa

Status of First Author: Student IN poster competition, PhD

Authors: Eliana Nossa, David Hysell, Miguel Larsen

**Abstract**: A new method to estimate the neutral winds for the Mesosphere and Lower Atmosphere region is presented. Using and inverse methods approach, the winds are estimated from the world day mode of the Arecibo incoherent scatter radar. The technique is compared with previous attempts to measure the neutral winds. Examples of the winds are estimated for couple of World Days. The estimated winds agree with previous observations, showing horizontal winds of around 100m/s and small vertical winds increasing at higher altitudes.

# ITMA-05 Study of vibrational-vibrational (V-V) energy exchange between CO2 isotopes in the middle and upper atmospheres of Earth and Mars - by Peter Panka

Status of First Author: Student IN poster competition, Masters

Authors: Peter Panka, Alex Kutepov, Erdal Yigit

**Abstract**: In the middle and upper atmospheres of Earth and Mars above about 90 km the local thermodynamic equilibrium (LTE) for vibrational degrees of CO2 molecules breaks down. The non-LTE significantly affects both radiation in the CO2 IR bands emitted from the atmosphere and the IR radiative cooling/heating of these atmospheric layers. Detailed accounting for non-LTE is needed for adequate diagnostics of the CO2 emission observations from space as well as for estimating the radiative cooling/heating in general circulation models (GCMs) involving MUAs. In this study we investigated intensive vibrational-vibrational exchange of energy by CO2-CO2 collisions. We found that this exchange leads to an effect similar to the source function equality in multiplets of atomic lines observed and analyzed in 1960s in stellar astrophysics. The discussion of how this effect can be applied for optimizing the non-LTE cooling/heating calculations is presented.

### ITMA-06 Multistatic Meteor Wind Radar and Results from a Recent Observation Campaign of the Geminids Meteor Shower in Adelaide, Australia by Cody Vaudrin

Status of First Author: Student IN poster competition, PhD

#### Authors: Cody Vaudrin and Scott Palo

**Abstract**: The Colorado Software Radar (CoSRad) comprises a fully functional FPGA-based softwaredefined radar remote sensing transceiver enabling the Multistatic Meteor Wind radar technique. CoSRad is a software configurable data acquisition system designed to operate over a wide range of radar remote sensing topologies. Ultimately, CoSRad endeavors to deploy a worldwide network of radars based on a common hardware platform and non-proprietary data processing techniques. CoSRad uses the directconvert receiver architecture to continuously sample eight antenna feeds and extract signals of interest from the resulting data stream. This poster presents a brief overview of the CoSRad hardware and software configured for multistatic specular meteor wind radar (MWR), followed by results from a recent measurement campaign in Adelaide, Australia. A CoSRad-based multistatic MWR was deployed and used to observe the Geminids meteor shower that peaked on Dec 14th, 2014. A multistatic MWR is defined by two or more geographically distributed (over 100's of km) receiver stations as opposed to the traditional MWR where the transmitter and a single receiver are co-located. Multistatic MWR is different from the traditional multistatic meteor radar where closely spaced stations (10's of km) are used to observe scatter simultaneously from the same trail for meteor orbit determination purposes.

This poster briefly outlines meteor trail forward-scatter theory. A population of example backscatter and forward-scatter echoes are presented as observed by both geographically distributed stations used in this multistatic experiment. A technique for meteor radar interferometer calibration is presented and various visualizations are used to exemplify the interferometric direction-of-arrival technique. Trail echo rates are presented between the forward and backscatter stations, and the inter-station echo rates are compared with those expected from the trail scattering theory and assumed meteoric trajectory distributions associated with the Geminids meteor shower. The poster discusses how this measurement campaign has laid the foundation for multistatic MWR's potential to improve the mesospheric wind field estimate and provide new experimental insight into meteor trail scattering and trail diffusion processes.

### ITMA-07 Low-cost Airglow Imager: Integrating CEDAR Science Into the Undergraduate Research and Course Curriculum - by Stuart Johnson

Status of First Author: Student IN poster competition, Undergraduate

Authors: Stuart Johnson, Josh Childs, Jared Pugh, Brian Patchett, Kim Nielsen

Abstract: Undergraduate research experience is arguably the most efficient form of high-impact learning and provides a solid foundation to be successful in graduate school. However, the majorities of undergraduate research activities are faculty driven, and while activities such as data acquisition and analysis as part of a faculty research projects are valuable, they miss the targets of high-impact learning: "The goal is to involve students with actively contested questions, empirical observation, cutting-edge technologies, and the sense of excitement that comes from working to answer important questions." (Association of American Colleges and Universities.) CEDAR is an excellent venue for undergraduate students to participate in as it incorporates multiple subjects of physics, and students can actively participate at any level. As an example, we present a student-driven project involving an airglow imaging instrument. With the recent development of low-cost and light-sensitive amateur astronomical CCD's, it is now possible to construct low-cost airglow imaging systems. During the 2015 spring semester, students at Utah Valley University constructed such a system and obtained first-light measurements in April. The system enables student hands-on experience with optical systems and provides students with excellent research opportunities to explore CEDAR science by defining their own projects. Furthermore, the instrument integrates into the physics curriculum at UVU, as it is an integral component of three courses: Optics, Geophysical Fluid Dynamics, and Basic Space Plasma.

This presentation shows the student progress in constructing the instrument and obtaining inaugural data, its role in student-driven research projects, and its implementation into the curriculum.

### Data Management

### DATM-01 Online Monitoring System for Lidar Operations and Data Handling at ALO-USU - by Luis Navarro Dominguez

Status of First Author: Student NOT in poster competition, Undergraduate

Authors: Luis A. Navarro, Vincent B. Wickwar, Marco A. Milla, Jose Gamboa

**Abstract**: The Rayleigh-scatter Lidar Group in the Center for Atmospheric and Space Sciences (CASS) at Utah State University (USU) has been developing and operating Rayleigh lidars since 1993 at the Atmospheric Lidar Observatory (ALO-USU) to study the middle atmosphere. To obtain the best scientific results, the system, both hardware and software, has been improved many times over this period and is still being improved. Because of these changes, we need to keep careful track of what software applies to what data. In addition, many funding agencies and journals now require establishing methodologies to preserve data and to keep track of the data used in specific projects and publications. To cope with these requirements, we have built three interconnected data structures to organize and manage the different data-acquisition hardware and software set-ups, and to keep track of the products generated by these. These data structures can all be managed from the internet. They were developed under the Django web framework and interconnect with other informatic tools such as Celery and MySQL to make it possible to handle a large volume of data. Moreover, even though this was developed for the ALO-USU Rayleigh lidars, it can be adapted to the needs of other lidar groups.

### Long Term Variations of the Mesosphere and Lower Thermosphere

### LTVM-01 27-day oscillation in the mesopause temperature observed by VHF meteor radar at King Sejong Station (62.2S, 58.8W), Antarctica - by Jeong-Han Kim

Status of First Author: Non-student, PhD

Authors: Jeong-Han Kim, Junseok Hong, Yong Ha Kim, Geonhwa Jee, Eswar Sunkara, Changsup Lee

**Abstract**: We have been operating VHF meteor radar at King Sejong Station (62.2S, 58.8W), Antarctica since March 2007, in order to measure neutral winds and temperatures in the polar MLT region. The mesospheric temperature inferred from meteor decay times observed by the VHF meteor radar is used to study the characteristics of the mesospheric temperature variations in the high-latitude region during the period from March 2007 to 2014. The results of the analysis showed that there is a 27-day oscillation in the meteor radar data, which is also confirmed from the Aura/MLS temperatures during the same period. We will also present the results of the comparison between the observation and the WACCM simulation for mesopause temperature and the discussion will be presented regarding the underlying physics.

### LTVM-02 Temperature responses to the 11-year solar cycle in the mesosphere and lower thermosphere from the 31-year (1979-2010) extended Canadian Middle Atmosphere Model simulation - by Quan Gan

Status of First Author: Non-student, PhD

Authors: Quan Gan, Jian Du, Victor I Fomichev, William E Ward, Stephen R Beagley, Shaodong Zhang, Jia Yue

Abstract: A recently nudged extended Canadian Middle Atmosphere Model run from 1979 to 2010 (eCMAM30) is used to investigate the zonal mean temperature response to the 11-yr solar cycle for the first time, with an emphasis on the mesosphere and lower thermosphere (MLT) region. We validate the modeled temperature response with results from the Halogen Occultation Experiment (HALOE) and the Sounding of the Atmosphere using Broadband Emission Radiometry (SABER) satellite observations in literature. The results show that eCMAM30 reasonably reproduces the amplitudes and latitudinal structures of the annual mean response in the lower and middle mesosphere when compared to HALOE. The annual mean responses are generally weaker by a factor of 2-3 than those from SABER observations in the whole MLT domain. However, the latitudinal structures and seasonal variations are in good agreement with SABER observations in the upper mesosphere and mesopause region. eCMAM30 exhibits an alternate structure with upper stratosphere warming and lower mesosphere cooling at NH middle latitudes in December, which is consistent with long-term Rayleigh lidar observations. In the NH polar region during February, eCMAM30 simulates a remarkable dipole structure with warming in the stratosphere and cooling in the mesosphere during solar maximum. Detailed examination of the dynamical processes suggests that the temperature response in the NH winter results from anomalous meridional residual circulation driven by planetary/gravity wave - mean flow interactions.

### Meteor Science other than Wind Observations

### METR-01 Dayglow from Atomic Nickel - by W.F.J. Evans

Status of First Author: Non-student, PhD

Authors: E.J. Llewellyn and Scott Budzein

**Abstract**: Day airglow from atomic nickel has been detected in RAIDS and OSIRIS satellite observations. The altitude profile was measured from 90 to 160 km.. This is the first observation of Ni in dayglow and supports the detection of Ni by LIDAR (Collins et al,2014). The relationship to Nickel Iron meteorites is discussed.

### METR-02 High-Altitude Radar Meteors Observed at Jicamarca Radio Observatory using Multi-Baseline Interferometric Technique - by Boyi Gao

Status of First Author: Student IN poster competition, Masters

Authors: Boyi Gao and John D. Mathews

**Abstract**: A new unambiguous, multi-baseline interferometric technique was recently employed for meteor observations at Jicamarca Radio Observatory (JRO). These observations largely confirm High-Altitude Radar Meteors (HARMs). The 50 MHz JRO array is arranged contiguous quarter-arrays (Q) each of which is comprised of 4×4 sub-arrays (M), which are referred to as square modules in Ochs' manual [Ochs, 1965]. In these observations the radar transmission was from two quarter-arrays sharing a common diagonal. Signal reception was via three quarter-array (Q) receivers and three adjacent (M) module receivers all of the same polarization. This arrangement offered the usual Q-Q and M-M interferometric baseline-pairs as well as new Q-M baselines that were rotated ~6° from the Q-Q and M-M baselines. For relatively high signal-to-noise ratio (SNR) meteors, this arrangement yielded ambiguity resolution to the horizon and confirmed the existence of HARM events. We report results from 4-5 August 2014 observations that include interesting new HARM events. We hope to extend this new technique with yet more baselines and higher sensitivity in near future observations.

### METR-03 Understanding the atmospheric and Ionospheric response to hypersonic objects in the Earth's atmosphere - by Robert Anthony Haaser

Status of First Author: Non-student, PhD

#### Author: Robert A. Haaser

Abstract: The goal of this project is to provide an absolute measurement of the Ionospheric and atmospheric perturbations from hypersonic objects in the atmosphere by associating the response with verifiable incoming objects. This work will advance the knowledge of phenomena associated with highvelocity objects in the atmosphere above 15 km by developing an empirically-based model that describes the characteristics and magnitudes of atmospheric perturbations generated by such bodies. The model will describe the effects of the body's velocity, altitude, and entry angle on resulting perturbations. GPS-derived total electron content (TEC) data, ground-based infrasound, and ionosondes will be used to monitor the Ionospheric and atmospheric response to such objects based on catalogued evidence from many real-world cases, such as the Space Shuttle re-entry and the Chelyabinsk bolide of 15 February 2013. LANL's experience and techniques will be used in measuring gravity waves and acoustic waves from GPS TEC ground-based and on-orbit measurements to monitor the F-region (200-400 km) Ionospheric response to the extraterrestrial objects. The E-region (100-150 km altitude) plasma response will be monitored by publiclyavailable ionosonde data. LANL's experience in infrasound detection will be used to monitor the response of the neutral atmosphere. Characteristics of incoming high-velocity objects will be collected from all available data sources (wide aperture radars, Doppler sounders, and fireball/bolide databases). The project will use relevant data from other observing modalities e.g. all-sky optical cameras, on-orbit optical sensors, and seismic arrays, as appropriate. Finally, this work will validate the empirically-based model developed from extensive case studies by extending models already available at LANL for atmospheric gravity waves, infrasound ray tracing and source detection to understand atmospheric pressure effects from these objects. An electrodynamic model that includes the coupling between neutral pressure waves and the charged ionosphere to understand associated plasma perturbations will be developed based on existing neutral wave models. Preliminary results will be presented, demonstrating progress toward project goals and describing how methodologies are applied to a few case events.

### METR-04 Measurements of Hypervelocity Impact Plasma Using a Plasma Spectrometer by Ashish Goel

Status of First Author: Student IN poster competition, PhD

Authors: Ashish Goel, Paul M. Tarantino, David S. Lauben, Andrew Nuttall, Yayu Monica Hew, Ivan Linscott, Sigrid Close

Abstract: Meteoroids and orbital debris are important components of Earth's space environment. Traveling at speeds up to 72 km/s, when these hypervelocity particles impact satellites in space, they vaporize, ionize and produce a radially-expanding plasma plume. This plasma can trigger electrostatic discharge events on satellites with differentially charged surfaces and the associated electromagnetic emission can also lead to electrical anomalies on satellites. In order to characterize the properties of this impact plasma, hypervelocity impact tests were carried out at the Colorado Center for Lunar Dust Acceleration Studies (CCLDAS) in Boulder, Colorado and at the Ames Vertical Gun Range (AVGR) facility in NASA Ames Research Center. At CCLDAS, low mass (0.1-340 fg) and high speed (15-100 km/s) projectiles were shot at a tungsten target and at AVGR, low speed (~6 km/s) and high mass (~6 mg) particles were shot at a copper target, allowing us to probe the physics of these plasmas across multiple mass-velocity regimes. The energy distribution and particle flux for biased and unbiased targets were measured using a multi-channel transient plasma analyzer (TPA) developed in-house at Stanford University. At CCLDAS, it was found that for biased targets, the cone angle of plasma expansion increases as the bias on the targets decreases, allowing us to estimate the thermal expansion speed of the constituents of the plasma. At AVGR, we were able to measure the flux of ions and electrons simultaneously across 16 energy channels, allowing us to estimate their energy distribution. These results offer new insights into the physics of hypervelocity impact plasmas and also prove the worthiness of the TPA in carrying out measurements of space plasmas. The TPA can be used on space missions in the future to detect and characterize meteoroid and orbital debris impacts, thereby improving our understanding of the mass, velocity and composition of these hypervelocity particles.

### METR-05 Time-resolved Emission Characteristics of Hypervelocity Impact Generated Flash - by Yayu Monica Hew

Status of First Author: Student IN poster competition, Masters

Authors: Yayu Monica Hew, Sirgrid Close, and Ivan Linscott

**Abstract**: Meteoroids and orbital debris, collectively referred to as hypervelocity impactors, travel between 7 and 70 km/s in free space. Upon their impact onto the spacecraft, the energy conversion from kinetic to ionization/vaporization occurs within a very brief timescale and results in a small and dense expanding plasma with a very strong optical flash alongside. This plasma can produce radio frequency (RF) emission that could potentially lead to electrical anomalies within the spacecraft. Additionally, space weather, such as solar activity and background plasma, can set up spacecraft conditions that can amplify the damages done by these impacts.

In this poster, we will present the optical data from our recent hypervelocity impact (HVI) experiment at the 3 MV electrostatic dust accelerator at the Colorado Center for Lunar Dust and Atmospheric Studies (CCLDAS). The facility is capable of accelerating micron or sub-micron charged particle to various velocities from 5 km/s to 100 km/s, which resemble the impact condition in free space. The optical sensor suite consists of three photomultiplier tubes (PMT) with three different interference color filters, i.e. 450 nm, 550nm, and 600 nm. Using the three-color PMT setup, we are able to achieve a time-resolved emission spectroscopy on the impact-generated flash. The spectroscopic data have revealed a near continuum emission spectrum. By blackbody radiation approximation, we can estimate the impact generated gas cloud/plasma temperature via Plank's formula. However, the spectrum experiences a less than blackbody like emission spectrum in parts of the time window. An optical model is thus derived to explain the time dependent behavior of the emission spectrum by considering possible emission and absorption effects in the impact generated plasma, i.e. free-free emission, free-bond emission, line radiation, Pseudocontinum effects. This work facilitates the understanding of hypervelocity impact generated plasma by connecting the impact generated flash with the plasma properties, i.e. temperature. Additionally, this optical method affords a less intrusive detection when compared to traditional plasma sensors, which might distort the electromagnetic fields around the plasma.

### METR-06 Accurate Detection of Micro-Meteor Observations by the Arecibo 430 MHz Incoherent Scatter Radar - by Daniel Kellett

Status of First Author: Student IN poster competition, Undergraduate

Authors: Daniel Kellett, Qihou Zhou, Mike Sulzer

**Abstract**: This poster focuses on accurate detection of meteor events and velocities by the Arecibo Observatory (AO) radio telescope. The operating frequency used is 430 MHz with a gate width (gw) of 1  $\mu$ s. Potential meteor events were determined by examining the signal to noise ratio (S/N) and, if large enough, examining other parameters such as the length of spike. We will report various meteor statistics including height, velocity, and local time.

### METR-07 Multi-instrument detection of meteoroids and ablation characterization by Lorenzo Limonta

Status of First Author: Student IN poster competition, Masters

#### Authors: Lorenzo Limonta, Glenn Sugar, Robert Marshall, Sigrid Close

**Abstract**: Optical and radar mass determinations are fraught with error due to difficulty in assessing the luminous efficiency (for optical) and the ionization probability (for radar), both of which depend on meteor velocity, composition, and other parameters. In the poster we propose an automated algorithm for dual detection of meteoroid from optical and radar measurements obtained at the Poker Flat facility. From

coincident detection of events we proceed on characterizing the relationship between optical and radar masses based on the relationship between the luminosity efficiency and ionization probability parameters

### METR-08 Spectra of Full 3-D PIC Simulation of Evolving Meteor Trails by Liane Kathryn Tarnecki

Status of First Author: Student IN poster competition, Undergraduate

#### Authors: Liane K. Tarnecki and Meers M. Oppenheim

**Abstract**: Radars detect plasma trails created by the billions of small meteors that impact the Earth's atmosphere daily, returning data used to infer characteristics of the meteoroid population and upper atmosphere. Researchers use models to investigate the composition and evolution of the meteors and plasma trails. In this paper, we examine spectra from full 3D simulations of meteor trail evolution under a variety of conditions. We also simulate meteors having a range of sizes as well as a range of ablation altitudes and atmospheric states. We compare the models to spectra from radar observations. The results of this study will allow more detailed and accurate information about the meteors to be drawn from non-specular radar observations of the trails, and aid in identifying the characteristics of the meteors that are best described by the simulations.

### METR-09 High spatial and temporal resolution radar measurements of meteor fragmentation at the Jicamarca Radio Observatory - by Qian Zhu

Status of First Author: Student IN poster competition, Masters

Authors: Qian Zhu, Ryan Volz, Ross Dinsmore, John Mathews

Abstract: Although meteoroids fragmentation has been observed and studied in the optical meteor community since the 1950s, no definitive fragmentation mechanisms for relatively faint meteors have been proposed, especially for gross fragmentation, due to the lack of observations to constrain the physical models. And it is challenging to record faint optical meteors while observing faint meteors using High-Power, Large Aperture (HPLA) radars yields considerable micrometeoroid fragmentation information especially while employing interferometric imaging. Interferometric imaging can potentially resolve the fragmentation process in three spatial dimensions while monitoring the evolution of the plasma in the headecho, flare-echo, and trail-echo regions of the radar meteor. That is, by tracking fragment and flaring radarechoing (plasma) regions with both high temporal and spatial resolution, we can improve understanding fragmentation mechanisms of micrometeoroids and the interactions between micrometeoroids and the atmosphere as well as inferring something of the micrometeoroids structure and composition. We present results of applying a newly-developed hybrid compressed sensing and holographic imaging technique to radar meteor observations conducted at the Jicarmaca Radio Observatory (JRO) in Peru. With the newly developed signal processing method—which provides improved temporal, Doppler, and spatial resolution over earlier techniques—we analyze five meteoroid fragmentation events. Results include observations of transverse spreading of the developing plasma apparently caused by gross fragmentation and plasma diffusion parallel to the geomagnetic field at the geomagnetic equator.

### METR-10 Characterization of Non-Specular Meteors Detected by a Non-Equatorial Radar - by Ana Maria Tarano

Status of First Author: Student IN poster competition, Masters

### Authors: Ana Maria Tarano, Diego Janches, and Sigrid Close

**Abstract**: Meteoroids entering the Earth's atmosphere are detected by radars as they ablate between 140 and 70 km altitude in the E-region of the ionosphere. The radar returns are classified as head echoes, plasmas surrounding the meteoroids, and trails, the expanding plasma column left in the meteoroid's wake.

Plasma trails are further categorized according to the angle between the meteoroid's trajectory and the radar beam. Non-specular trails are returns from meteoroids traveling quasi-parallel to the radar beam while specular trails travel perpendicular to the beam. Literature and models state that in order to detect non-specular trails, the radar beam must be quasi-perpendicular to the Earth's magnetic field with aspect angle sensitivities of 1-2 degrees to reflect from field aligned irregularities (FAI) after the onset of plasma turbulence.

However, the Southern Argentina Agile Meteor Radar (SAAMER) has surprisingly detected 25 cases of non-specular trails over a period of 12 days in 2011. At the radar's location, the background magnetic field is ~40 degrees off the radar beam and hence contradicts previous literature, which suggests that the meteor community is disregarding additional instabilities within the plasma. This poster will present on the interferometric results from observations performed with SAAMER in order to gain a better understanding of non-specular trail reflections. Moreover, comparisons of results from an equatorial radar will be presented in order to elucidate the cause of observations.

### METR-11 Weibel instability in meteoroid impact-produced plasmas - by Alex Fletcher

Status of First Author: Student IN poster competition, PhD

#### Authors: Alex Fletcher and Sigrid Close

**Abstract**: Meteoroids and interplanetary dust particles regularly strike spacecraft at speeds up to 72 km/s. These impacts are energetic enough to vaporize and ionize the projectile in its entirety as well as a portion of the spacecraft material, generating plasma that swiftly expands into the surrounding environment. Plasma is produced for speeds greater than ~8 km/s and that plasma expands in a fully ionized state for speeds greater than ~20 km/s. Using high-order particle-in-cell simulations, we show that this expanding plasma can develop a temperature anisotropy that triggers the Weibel instability. The danger that Weibel-generated magnetic fields might pose to the nearby spacecraft is also assessed. The simulations show the Weibel instability is a possible radiation mechanism for radio frequency emission that has been observed in ground-based impact experiments.

### METR-12 A Comparison of Optical and Radar Meteoroid Mass Estimates Using Simultaneous Observations - by Benjamin Thomas Spangler

Status of First Author: Student NOT in poster competition, Undergraduate

Authors: B. Spangler, M. Oppenheim, R. G. Michell, E. Fucetola, M. Samara, J. Chau, F. Galindo, M. Milla

**Abstract**: Each second the Earth's atmosphere is bombarded by millions of meteoroids, most of which have masses less than a milligram. As they ablate upon entry into Earth's atmosphere, the larger meteors are observable by optical instruments while the smaller ones are observable only by radars. This study examines combined optical and radar observations of the same five meteors. It compares a variety of independent methods of estimating the masses of these particles. Specifically, it studies an optical luminosity method and two radar methods: a simple, analytical deceleration model and a more complex ablation model. We will compare the mass estimates of each model and discuss possible reasons for any differences in estimates, as well as note the advantages and disadvantages of each mass estimation technique.

### **MLT Gravity Waves**

# MLTG-01 Ionospheric acoustic and gravity waves associated with mid-latitude thunderstorms - by Erin H. Lay

Status of First Author: Non-student, PhD

Authors: Erin H. Lay, Xuan-Min Shao, Alexander K. Kendrick, Charles S. Carrano

**Abstract**: Acoustic waves with periods between 2 and 4 minutes and gravity waves with periods between 6 and 16 minutes have been detected at ionospheric heights (250-350 km) using GPS Total Electron Content (TEC) measurements and associated with underlying thunderstorm activity. A statistical study comparing NEXRAD radar thunderstorm measurements with ionospheric acoustic and gravity waves in the midlatitude U.S. Great Plains region was performed for the time period of May - July 2005. Ionospheric acoustic wave area and ionospheric gravity wave area are clearly associated with thunderstorm size. For acoustic waves, the disturbed area and amplitude is associated with large mesoscale thunderstorms. Ionospheric gravity wave disturbed area and amplitude scale with thunderstorm activity.

### MLTG-02 Local Gravity Wave Effects on the DW1 Tidal Variability In WACCM/eCMAM - by Ryan Matthew Agner

Status of First Author: Student IN poster competition, PhD

Authors: Ryan M. Agner and Alan Z. Liu

**Abstract**: Gravity waves and atmospheric tides have strong interactions in the mesopause region and is a major contributor to short term variabilities of the tides in this region. Global Circulation Models (GCM's) can be used to study these variabilities. These global scale numerical models can directly simulate the tides but must have gravity waves parameterized due to their smaller spacial scales. In this work, the short term variability of the DW1 tide is investigated by considering the effects of local time diurnal variabilities due to gravity wave forcing. The variabilities are analyzed in the Whole Atmosphere Community Climate Model (WACCM) and the extended Canadian Middle Atmosphere Model (eCMAM) considering the effects of the different parameterization schemes and model resolutions. The contributions from large and small GW's are also analyzed.

### MLTG-03 The relative importance of temperature and wind medium scale wave perturbation fields in refracting small-scale gravity waves. - by Christopher Heale

Status of First Author: Non-student, PhD

Authors: Christopher J. Heale and Jonathan B. Snively

Abstract: Interactions between gravity waves of different scales are frequent in the upper atmosphere. LIDAR observations and OH airglow Keograms have revealed that larger scale and longer period waves modulate the background propagation environment for short period waves [e.g. Li et al 2007, Ramesh et al. 2013, Cai et al. 2014, Bossert et al. 2014]. It is suggested that these short period waves contribute a significant proportion of the MLT momentum flux [Fritts et al. 2014]. Numerical modeling and ray-tracing have been used to investigate interactions between waves of different scales in both the ocean and atmosphere [e.g. Broutman and Young 1985, Eckermann 1997, Sartelet 2003, Hasha and Buhler, 2008, Senf and Achatz 2011]. However, it is common to approximate the larger-scale waves as horizontallyhomogeneous spatially-periodic wind fields, or to neglect the interactions between small and larger scale waves. In this study, a combination of numerical modeling and ray-tracing is used to investigate the relative effects and importance of the temperature and horizontal wind perturbation fields of a medium scale  $(\lambda x \sim 100 \text{ km}, \text{ period } \sim \text{hours})$  wave on the refraction of a  $(\lambda x \sim 10 \text{ km}, \text{ period } \sim \text{minutes})$  small-scale wave in the atmosphere at non-breaking amplitudes. This is done for 1) a horizontally homogeneous case, 2) a horizontally inhomogeneous case, and 3) a fully nonlinear 2-D wave-wave interaction. We investigate the importance of including the wind and temperature perturbation quantities, and the validity of linear assumptions, to provide guidance for future modeling and observational studies.

### MLTG-04 Observational and Modeling Study of Gravity Wave Propagation Through Reflection and Critical Layers - by Bing Cao

Status of First Author: Student IN poster competition, PhD

Authors: Bing Cao, Alan Z. Liu, Christopher J. Heale and Jonathan B. Snively

**Abstract**: A gravity wave package propagating through two partial reflection and one critical layer was observed from 05:00 to 09:00 UTC on 16 January 2015 by a sodium lidar and an all sky airglow imager located at the Andes Lidar Observatory (ALO) in Cerro Pachón (30°14'S, 70°44'W), Chile, between 80 and 105 km. This gravity wave package has periods of 20-35 min and horizontal wavelengths of 40-50 km. Strong enhancement of vertical wind perturbations exceeding 10m/s amplitude is found below 90km, consistent with the wave behavior near a reflection layer. The reduction of vertical wavenumber is found near the critical layer. The background atmospheric stability also strongly influences wave amplitudes. A fully-nonlinear model was used to simulate this event and was able to reproduce most of the observed features, which provides more insights of this complex event.

# MLTG-05 The study of gravity wave components with different vertical scales in the stratosphere based on SABER temperature data - by Yun Zhang

Status of First Author: Non-student, PhD

Authors: Yun Zhang and Weixing Wan

Abstract: Global observations of gravity waves have been performed using the SABER/TIMED temperature data during the period from January 2002 to January 2012. Each temperature perturbation profile was analyzed using wavelet transformation to estimate the vertical wavelengths of gravity waves. We compared the global distributions of gravity wave potential energy obtained by two traditional methods of extracting gravity wave perturbations and then improved the methods by separating the different gravity wave components according to vertical scales to get a better insight into the final analyzed gravity wave parameters. Enhanced gravity waves at low latitudes in the summer hemisphere are mainly owing to components with moderate wavelength  $10 < \lambda z < 25$  km excited by deep convection and topographic sources, whereas those at middle and high latitudes in the winter hemisphere are predominantly attributed to waves with long wavelength  $\lambda z > 25$  km which are related to the spontaneous adjustment, equatorial convection and strong background winds. The temporal variation of equatorial gravity waves was analyzed. The OBO (quasi-biennial oscillation) feature appears in some parameters part results of the waves with short wavelength  $\lambda z < 10$  km and moderate wavelength  $10 < \lambda z < 25$  km in the lower stratosphere (about 20-30 km altitudes). Wave components with long wavelength  $\lambda z > 25$  km mainly reflect the characteristic of SAO (semi-annual oscillation) in the upper stratosphere (above 30 km). The AO (annual oscillation) in all components is prevalent at altitudes near 20 km.

### MLTG-06 Observation of mesospheric gravity waves with an All-Sky Camera in King Sejong Station, Antarctica (62° 13'S, 58° 47'W) - by Hosik Kam

Status of First Author: Student IN poster competition, Masters

Authors: Hosik Kam, Yong Ha Kim, Geon Hwa Jee, Young-bae Ham

**Abstract**: We have carried out all-sky imaging of OH Meinel airglow layers in the period from 2008 through 2014 at Korean Antarctic King Sejong Station(KSS). We analyzed the images observed during a total of 143 clear moonless nights and found 94 events of short period(<1hr) band-type waves. We determined wave characteristics such as horizontal wavelengths, phase speeds, periods and propagating directions of observed waves. We find that the wave propagation is preferentially westward and phase speeds tend to be relatively low in the westward waves. The anisotropy may relate to Antarctica Peninsula

because waves could be generated by orographic forcing, polar vortex, cold fronts or strong cyclonic activity over the Antarctica Peninsula. Furthermore, we derive intrinsic phase speeds and periods by using mean wind information from simultaneous observation of the KSS meteor radar. We discuss the observed and intrinsic wave properties by comparing with those observed from other Antarctic stations, such as Comandante Ferraz Station(62.1°S, 58.4°W), Halley Research Station(75.5°S, 26.7°W), Rothera Research Station(67.5°S, 68.4°W).

### MLTG-07 Gravity Wave Sources over South Pole - by Dhvanit Mehta

Status of First Author: Student IN poster competition, PhD

Authors: Dhvanit Mehta, Andrew Gerrard, Yusuke Ebihara, Allan Weatherwax

**Abstract**: We present gravity wave observations from mesopause 557.7-nm OI all-sky data taken by a multiwavelength all-sky imager located at South Pole, Antarctica. Focusing on gravity waves observed during the month of August, 2004, we investigate possible sources of observed waves using the FOREGRATS ray-tracing model. We note instances where the source region of waves coincide with regions of baroclinic instability by comparing gravity wave ray paths with ECMWF geopotential height maps of the polar vortex structure.

### MLTG-08 Investigating Thermospheric Gravity Wave Amplitudes in the High Arctic by Michael R. Negale

Status of First Author: Student IN poster competition, PhD

Authors: Michael R. Negale, Michael J. Taylor, Kim Nielsen, Michael J. Nicolls

**Abstract**: A majority of gravity waves are generated in the lower atmosphere. As they propagate upwards from their source regions, their amplitudes grow due to decreasing atmospheric density. At various regions in the atmosphere, the waves will begin to dissipate or break and deposit energy and momentum. Using the Poker Flat Incoherent Scatter Radar, we observed traveling ionospheric disturbances (TIDs) from August 2010 – April 2013. TIDs are known to be ionospheric manifestations of neutral thermospheric gravity waves. Therefore, through TID measurements, we can investigate the vertical and horizontal thermospheric gravity wave parameters as a function of altitude and time. For this presentation we present new results of the wave amplitudes deduced from the relative electron density perturbations as a function of altitude enabling us to investigate the regions where the waves dissipate and break.

### MLTG-09 Satellite measurements of mesospheric gravity wave temperature variances over the Andes - by Jonathan Pugmire

Status of First Author: Student IN poster competition, PhD

Authors: Jonathan Pugmire, Michael J. Taylor, Yucheng Zhao, James M Russell III

**Abstract**: Focusing on over 10 years of data from the SABER instrument aboard the TIMED satellite temperature variances are determined to quantify the signatures of short-period gravity waves propagating up into the mesosphere, and lower thermosphere (MLT) region. Temperature profile measurements were measured by SABER within a limited geographical area, centered on the Andes Lidar Observatory at Cerro Pachon, Chile (30.3° S, 70.7° S) where Utah State University has operated an OH Mesospheric Temperature Mapper (MTM) for the past 5 years. Using an established procedure the large-scale tidal waves, with wavenumbers 0-6, were removed from each profile revealing the gravity wave perturbations as a function of altitude. Computed temperature variances and potential energy reveal increased wave activity during the winter months, possibly due to mountain waves. The results are compared with the ground-based mesospheric temperature measurements. This technique has high potential for coordinates satellite and ground-based investigations of gravity wave effects from multiple sites around the world.

# MLTG-10 Horizontal phase speed distribution of gravity waves observed in mesospheric temperature maps - by Ahmad Talaei

Status of First Author: Student IN poster competition, PhD

Authors: Ahmad Talaei, Mike Taylor, Pierre-Dominique Pautet, Takashi S. Matsuda and Takuji Nakamura

Abstract: The goal of the current work is to develop a method suitable for analyzing the horizontal phase speeds of atmospheric gravity waves from an extensive amount of gravity wave data obtained by the USU Advanced Mesospheric Temperature Mapper (AMTM) from Antarctica. The AMTM is a novel infrared digital imaging system that measures selected emission lines in the mesospheric OH (3,1) band to create intensity and temperature maps of the mesosphere. This analysis builds on the recent work by Matsuda et al 2014 using all-sky intensity data to investigate the horizontal phase speed distribution. In our analyses we applied this technique to measure spectrum from temperature maps with more limited 120 degree field of view but 24 hr. measurements at South Pole. The ground-based remote sensing temperature measurements have been obtained using the nighttime hydroxyl (OH) emission, which originates at an altitude of  $\sim$ 87 km. The results are compared to intensity data and to conventional event analysis in which the phase fronts are traced manually.

# MLTG-11 Gravity wave activity over Chatanika, Alaska and its relationship to the wind field and geostrophic adjustment - by Colin Charles Triplett

Status of First Author: Student IN poster competition, PhD

Authors: Colin C. Triplett, Richard L. Collins, V. Lynn Harvey, Kim Neilsen, Kohei Mizutani

Abstract: The general circulation of the middle and upper atmosphere is determined by waves that form in the lower atmosphere. Large scale Rossby waves and small scale gravity waves propagate upward and release their energy in regions of instability such as critical layers. Rossby wave breaking leads to large scale disturbances in the wind and temperature fields know as a sudden stratospheric warming (SSW). These have a great impact on the seasonal weather and climate of the middle atmosphere. SSW events have a particular relationship with gravity waves in the Arctic middle atmosphere. During these events gravity waves help in the reestablishment of the geostrophic balance in the wind field, i.e. the stratospheric polar jet. This return to geostrophic balance, called geostrophic adjustment, will produce gravity waves itself. We want to look at how geostrophic adjustment affects wave energies seen in the Arctic. One metric used to explore geostrophic adjustment is the magnitude of the residual of the nonlinear balance equation (NBE). NBE is used because of close relationship to the primitive equations and its ability to capture the nonlinear processes that occur during geostrophic adjustment that other metrics, such as the Lagrangian Rossby number, can't resolve. We use a high quality subset of the data (152 nights) from the Lidar Research Laboratory (LRL) at Poker Flat Research Range (PFRR), Chatanika, Alaska (65 N, 147 W) to investigate the relative roles of both critical layer filtering and NBE generation of gravity wayes. These data are processed to look at energies in the 40-50 km region and then compared to the wind and NBE fields of the Modern Era-Retrospective analysis for Research and Applications (MERRA) reanalysis. The gravity wave energy and horizontal wind demonstrates are highly correlated, primarily with regions of the stratosphere with slow winds. The highest correlation of gravity wave energy with NBE occurs with NBE in the upper troposphere. We discuss the results in terms of recent case studies [Wang and Alexander, 2009] [Zhang et al, 2001].

### MLTG-12 Gravity Wave Parameter Distribution over multiple seasons using an All Sky Imager in Eureka, Nunavut, Canada - by Chris William Vail

Status of First Author: Student IN poster competition, Masters

#### Authors: Chris Vail and William Ward

**Abstract**: This poster will present the analysis approach developed to detect of gravity waves and the variation in gravity wave parameters deduced from the airglow images taken by the Polar Environmental Atmospheric Research Laboratory (PEARL) All Sky Imager (PASI). PASI has been in operation since November 2007 at PEARL in Eureka, Nunavut, Canada (located at 80N,86W) with images being taken on average every 45 seconds during the winter seasons. An automated data analysis approach has been developed to diagnose the gravity wave parameters in a time efficient manner.

PASI is a CCD imaging system with six different spectral band narrow band filters. The filters of interest in this research isolate the following airglow emissions: atomic sodium (at 589.3 nm), atomic oxygen green line (at 557.7nm), and hydroxyl (at 720-910nm notched at 865nm due to the molecular oxygen). PASI cycles through the different filters with the hydroxyl filter interleaved between the other filters in the sequence.

The gravity wave parameters to be presented are the horizontal and vertical wavelength, intrinsic period and propagation direction. In each image occurrences of these waves are defined in terms of horizontal spatial wavenumber and phase. Temporal frequency information is deduced from consecutive images which contain wave signatures with similar horizontal wavenumbers. The vertical wavelength is determined from consecutive images between the different airglow emissions using an approach similar to determining the temporal frequency.

This work will present monthly variations of these parameters along with their uncertainties for several seasons. In particular, the daily variance in gravity wave occurrence during Stratospheric warmings will be highlighted.

### MLTG-13 Statistical Study of High to Medium Frequency Mesoscale Gravity Waves over the Central US using Temperature Mapper, CRRL Na Lidars, and ECMWF by Haoyu Li

Status of First Author: Student IN poster competition, Undergraduate

Authors: Haoyu Li, Xian Lu, Xinzhao Chu, Wentao Huang, John Smith, Cao Chen, Tao Yuan, Pierre Dominique Pautet, Mike Taylor, Andreas Dörnbrack

Abstract: We present the first statistical study of the gravity waves with periods of 0.5-2 h observed by the coordinated two CRRL Na Doppler lidars at Boulder, CO (40.1°N,105.2°W) and Logan, Utah (41.7°N,111.8°W), and the temperature mapper at Logan, Utah. Due to the significant improvement of the receiver efficiency of the STAR lidar at Boulder, the vertical winds can now be directly measured with high temporal and spatial resolutions, from which the most dominant wave signatures are those with periods of 0.5-2 h. The coordinated case study in Lu et al. [2015] has developed a systematic method to fully characterize a mesoscale 1-h wave because the vertical-range-resolved lidar measurements can be used to provide the vertical information of waves and background winds, while the horizontal-rangeresolved temperature mapper can be used to derive wave horizontal structure. Since these waves are frequently observed over Boulder and Logan, and are the dominant features in the vertical winds, we perform a statistical study of the these waves by following the method of Lu et al. [2015]. The intermittency of the waves is studied by counting the number of wave events in the observational database. The statistical distributions of the horizontal and vertical wavelengths, azimuth and elevation angles of wave propagations, intrinsic periods, and group velocities are revealed. In particular, the combined lidars and mapper measure the wave amplitudes in the four elementary parameters, which are temperature, zonal, meridional and vertical winds. These enable us to also characterize the distribution of wave amplitudes in

these physical quantities. By using the ECMWF data, we establish the vertical wave propagations for some of the cases by identifying the waves with nearly the same horizontal structure and suggest possible wave sources. (40.1°N,105.2°W) and Logan, Utah (41.7°N,111.8°W), and the temperature mapper at Logan, Utah. Due to the significant improvement of the receiver efficiency of the STAR lidar at Boulder, the vertical winds can now be directly measured with high temporal and spatial resolutions, from which the most dominant wave signatures are those with periods of 0.5-2 h. The coordinated case study in Lu et al. [2015] has developed a systematic method to fully characterize a mesoscale 1-h wave because the verticalrange-resolved lidar measurements can be used to provide the vertical information of waves and background winds, while the horizontal-range-resolved temperature mapper can be used to derive wave horizontal structure. Since these waves are frequently observed over Boulder and Logan, and are the dominant features in the vertical winds, we perform a statistical study of the these waves by following the method of Lu et al. [2015]. The intermittency of the waves is studied by counting the number of wave events in the observational database. The statistical distributions of the horizontal and vertical wavelengths, azimuth and elevation angles of wave propagations, intrinsic periods, and group velocities are revealed. In particular, the combined lidars and mapper measure the wave amplitudes in the four elementary parameters, which are temperature, zonal, meridional and vertical winds. These enable us to also characterize the distribution of wave amplitudes in these physical quantities. By using the ECMWF data, we establish the vertical wave propagations for some of the cases by identifying the waves with nearly the same horizontal structure and suggest possible wave sources.

### MLTG-14 Undergraduate High Impact Learning Through Ray Tracing of Atmospheric Gravity Waves - by Johnathon S. Gay

Status of First Author: Student IN poster competition, Undergraduate

Authors: Johnathon Gay and Kim Nielsen

**Abstract**: Undergraduate students often engage in research activities that are part of a larger project outlined by research faculty, while it is less common for students to explore and define their own research project. The later has been shown to have tremendous impact on the learning outcome of the students and provide a stronger sense of pride and ownership of the research project. It is unrealistic to expect starting undergraduate students to define transformative research projects. However, with the proper training and guidance student-driven transformative research is possible for upper division students. We present here a project that engage students in aeronomy research activities and provide them with a base to establish their own research projects for senior year.

The starting point is in observed atmospheric gravity waves in the mesosphere. While these waves have been observed and studied in details for decades, there are still many questions to be addressed with respect to their propagation from the lower atmosphere into the mesopause region. The project presented here demonstrates the progress of a simple reverse ray tracing model to propagate the observed wave downwards through the atmosphere to its point of origin. In this process, we build a numerical model based on basic calculus taught in introductory calculus courses and a simple dispersion relation for wave motion in a stable atmosphere.

### MLTG-15 Detection and estimation of Gravity Wave parameters from the Jicamarca All-Sky Imager - by Luis Navarro Dominguez

Status of First Author: Student NOT in poster competition, Undergraduate

Authors: Luis A. Navarro, Michael J. Taylor, Vincent B. Wickwar, Pierre-Dominique Pautet, Fabio Vargas, Gary R. Swenson, Marco A. Milla

**Abstract**: In the mesosphere and lower thermosphere, there are several phenomena caused by altitudedependent perturbations such as gravity waves. They are mechanical waves that propagate upward transferring energy from one atmospheric level to the next. It is possible to detect their presence by using passive optical instrumentation with the appropriate optical filters as in the Jicamarca All-Sky Imager (JASI).

The JASI (11°57'30"S, 76°51'33"W) is collocated with the Jicamarca Radio Observatory and the Jicamarca Fabry-Perot Interferometer. Its optical design, consisting of a telecentric lens, a fish-eye lens, and an interference filter with a passband from 750 nm to 930 nm and a blocking filter at 865 nm to avoid an O2 emission, enables the imager to observe the OH Meinel bands originating from excited neutral OH between 85 km and 90 km in the upper mesosphere and lower thermosphere.

Later, a set of routines is applied to the images to detect and estimate the gravity wave parameters. The images are initially preprocessed, removing background (background wind, stars and milky way) and performing a spatial calibration. Then a phase-difference algorithm is applied to the time-differenced images to derive the gravity wave parameters: the horizontal and vertical wavelengths, phase speed, period, direction of propagation, amplitude, and momentum flux. By following this new set of procedures, it is possible to analyze gravity wave activity in the mesosphere using the Jicamarca All-Sky Imager.

### MLT Lidar Studies

# MLTL-01 The transition from summer-to-winter temperatures between 70 and ~115 km as observed with the ALO-USU Rayleigh lidar - by Vincent B. Wickwar

Status of First Author: Non-student, PhD

Authors: Vincent B. Wickwar, Leda Sox, Matthew T. Emerick, Joshua P. Herron, David L. Barton

**Abstract**: Rayleigh-scatter lidar observations were made at the Atmospheric Lidar Observatory (ALO) at Utah State University (USU) from 1993–2004 from 45–90 km. The lidar operated at 532 nm with a power-aperture-product (PAP) of ~3.1 Wm2. The sensitivity of the lidar has since been increased by a factor of 66 to 205 Wm2, extending the maximum altitude into new territory, the lower thermosphere. Observations have been extended up to 115 km, almost to the 120 km goal. Early temperatures from ~4-week periods starting in June 2014 are presented and discussed. They are compared to each other, to the ALO climatology from the original lidar, and to temperatures from the NRLMSISe00 empirical model. They clearly show the complex transition from summer winter. At the lower altitudes they mostly show similarities to the original ALO-USU climatology. They show similarities and differences with the NRLMSISe-00 temperatures.

### MLTL-02 Stratospheric and MLT Temperature and Horizontal Wind Vector Collection Using Na-DEMOF Receivers - by Ian Barry

Status of First Author: Student IN poster competition, Masters

Authors: Ian Barry, Wentao Huang, John Smith, Xinzhao Chu

**Abstract**: Derivation of temperatures and vertical winds in the lower and middle atmosphere using a sodium Double-Edge Magneto-Optic Filter (Na-DEMOF) has previously been demonstrated up to an altitude of 70 km using a zenith-pointing beam and telescope. This poster marks the expansion of these results to derivation of horizontal wind vectors through the use of two beams and receivers pointed toward the North and West at 70° elevation angles. The final poster will highlight phenomena observed in the collected data, and show the receiver design in detail. The procedure for calibrating the filter using zenith-pointing data and assumption of zero-mean winds will also be presented. The expansion of the capabilities of the STAR Na Doppler lidar to horizontal wind derivation in the lower atmosphere allows for study of horizontal gravity wave propagation.

### MLTL-03 Instabilities, Critical Layers, and Secondary Gravity Wave Generation in the Mesosphere and Lower Thermosphere During the DEEPWAVE Campaign by Katrina Bossert

Status of First Author: Student IN poster competition, PhD

Authors: Katrina Bossert, David C. Fritts, Bifford P. Williams, Pierre-Dominique Pautet, Michael J. Taylor

**Abstract**: Certain background conditions within the Mesosphere and lower Thermosphere (MLT) generate environments under which instabilities and critical layers occur for various spectra of gravity waves. These conditions can lead to gravity wave breaking, resulting in momentum deposition and the generation of secondary gravity waves that also transport momentum within the MLT. Momentum transport and deposition can have strong implications within the MLT, including induced drag on zonal and mean winds. Given the important role gravity waves play in momentum transport, a better understanding of the conditions leading to instability, gravity wave breaking, and secondary gravity wave generation is necessary for improving our predictive capabilities of gravity wave influences on the momentum budget of the MLT within models. This poster examines instances of observed gravity wave instability and breaking events leading to secondary gravity wave generation within the MLT during the DEEPWAVE campaign, and the background atmospheric conditions contributing to these events.

## MLTL-04 A statistical study of the 4-9 h waves in the Antarctic middle and upper atmosphere observed by lidar - by Cao Chen

Status of First Author: Student IN poster competition, PhD

Authors: Cao Chen, Xinzhao Chu, Xian Lu, Weichun Fong

**Abstract**: Since the start of the McMurdo Fe lidar campaign, large-amplitude (~±30 K), long-period (4 to 9 h) waves with upward energy propagating signatures are frequently observed in the MLT temperatures at McMurdo (77.8°S, 166.7°E). Despite its frequent appearance, such type of wave was neither widely observed nor well understood in the past. Particularly, the persistent appearance and long lifetime of these waves contradicts the current understanding of Gravity Waves being intermittent due to intermittency in wave sources (both spatial and temporal), in wave dissipation and randomness in wave propagating inside or outside the observation range.Therefore, the observations of these 4-9 h waves at McMurdo has suggested either persist wave source(s), or favorable propagation conditions or largeness in scales of the waves. We utilize lidar temperature data in winter (May, June, and July) from 2011 to 2014, to derive several statistical wave properties of these 4–9 h waves, such as dominant periods, vertical wavelengths, amplitudes and phases. This will help us obtain a more comprehensive interpretation of the waves and also help us in identifying the wave sources.

### MLTL-05 Sodium observation in the lower thermosphere (120-160 km) at the Andes Lidar Observatory - by Yafang Guo

Status of First Author: Student IN poster competition, Masters

Authors: Yafang Guo, Alan.Z.Liu, Fabio Vargas, Anthony Mamgognia, Gary R. Swenson

**Abstract**: Na Lidars normally observe the neutral sodium atoms in the 80-105 km altitude region, produced by the meteoric ablation. There are some limited observations of Na above 110 km. This work reports recent Na Lidar observations of high altitude Na at the Andes Lidar Observatory, located at Cerro Pachón, Chile (30.0°S, 71.0°W) since May 2014. Out of 27 nights of observations in April, May, August and September, Na were observed at up to 160 km altitude on 11 nights. The peak Na density at 120 km altitude is about 10 atoms /cm^3, about 0.1% of the peak density around 92 km. The observed Na density on all nights show a common structure of downward progression, which is indicative of possible tidal influence. On one night (Sep 9, 2014), two bands of this downward progressing Na were observed, with an

interval of about 8 hours. Temperatures were also derived in this altitude range when Na was present. Possible influence of terdiurnal tide was explored.

### MLTL-06 Changing Atmospheric Composition and the Retrieval of Rayleigh Lidar Temperatures in the Lower Thermosphere - by Leda Sox

Status of First Author: Student NOT in poster competition, PhD

#### Authors: Leda Sox and Vincent B. Wickwar

Abstract: Rayleigh-scatter lidar measurements have provided relative density and absolute temperature measurements of the middle and upper atmosphere (~35-90 km) for over three decades. The data acquired with these instruments have been used to study the thermal structure, dynamics and long-term trends in these atmospheric regions. Recently, the Rayleigh lidar on the campus of Utah State (42°N, 112°W) has been upgraded to include more transmitted power (42 W) and a larger receiving aperture (4.9 m2), which has enabled observations to be regularly made from 70 to above 110 km. Inherent in the current Rayleigh lidar temperature retrieval methods is the assumption that the neutral atmosphere is a turbulently mixed combination of molecular oxygen (O2), nitrogen (N2) and atomic argon (Ar), which is a good assumption up to about 95 or 100 km. This assumption allows one to take the Rayleigh-backscatter crosssection (RBCS) and mean molecular mass (MMM) to be constant over the altitude range of the Rayleigh lidar measurements, which previously did not extend above 90 km. However, above 100 km, photodissociation breaks up molecular oxygen to form a layer of atomic oxygen (O) along with the mixture of N2, O2 and Ar. Due to this change in atmospheric composition, the temperature retrieval method used for new Rayleigh lidar measurements above 100 km must be amended. In this work, we will make corrections to the Rayleigh lidar temperature algorithm in order to account for changing RBCS and MMM with altitude. The corrections will be developed using the NRLMSISe00 empirical model and will then be applied to the USU Rayleigh lidar data obtained over the past year.

### MLTL-07 Design and implement a new Na Faraday filter for STAR Na Doppler lidar at Boulder to make high-quality daytime measurements - by Wentao Huang

Status of First Author: Non-student, PhD

Authors: Wentao Huang, John A. Smith, Xinzhao Chu, Ian F. Barry, and Jian Zhao

**Abstract**: A new Na Faraday filter has been designed and constructed for 3-frequency Na Doppler lidar. This filter features a wider transmission peak around the Na D2a transition frequency than other Faraday filters currently in use. Such improvement is realized by the combination of a stronger magnetic field (~2350 Gauss) and proper Na vapor pressure. Using Zemax, we designed the daytime receiver for the STAR Na Doppler lidar at Boulder, and optimized the optical efficiency. Our sky tests on April 29th 2015 demonstrated daytime Na resonance signal level of 250 counts per shot for the whole Na layer with 10 mJ transmitted power at the peak frequency. The solar background reached maximum about 120 counts/24-m bin/300 shots between noon and 1 pm local time. The signal to noise ratio was about 9 when the solar background was highest. Compared with daytime measurements from other Na Doppler lidars, such significantly improved signal level will provide new opportunities to investigate the processes in Mesosphere and Lower Thermosphere (MLT) region that previously difficult to be resolved because of the low signal level and the relatively high solar background.

### Mesosphere or Lower Thermosphere General Studies

MLTS-01 CO2 in the MLT: constraining the CO2(v2)-O quenching rate coefficient - by Erin Dawkins

Status of First Author: Non-student, PhD

Authors: E. Dawkins, D. Janches, A. Kutepov, A. Feofilov, A. Panka

**Abstract**: Carbon dioxide plays an important role in the terrestrial atmosphere, with infrared emission in the 15  $\mu$ m CO2 band (115 $\mu$ m) providing the dominant cooling mechanism in the mesosphere/lower thermosphere (MLT) region via interaction with atomic O. This CO2(v2)-O quenching rate coefficient is poorly understood and current estimates vary by a factor 3-4, with a significant discrepancy between laboratory measurements and those provided by satellite remote sensing. However, the true value of this rate coefficient is of vital importance in understanding both the energetics of the MLT region and for temperatures retrievals from measurements of 115 $\mu$ m.

This work proposes to build upon and extend an existing methodology developed by Feofilov et al. (2012) who used TIMED/SABER satellite instrument data to retrieve the CO2(v2)-O quenching rate coefficient using a synergy of atmospheric and ground-based lidar temperature measurements. Current work involves assessing whether there is a spatio-temporal variability component to this rate coefficient, and what this could reveal about whether there are additional relevant energy sources and sinks in the real atmosphere that are not currently reproduced under laboratory conditions.

### MLTS-02 Investigation on how the strong Sporadic Na layer formed by model simulation by Xuguang Cai

Status of First Author: Student IN poster competition, Masters

Authors: Xuguang Cai and Tao Yuan

**Abstract**: The high altitude sporadic Na layer events around the globe have drawn considerable attention lately due to its possible role as a resonance lidar's tracer for the measurements of thermospheric temperature and wind. Recent studies have demonstrated that the major source of the sporadic Na layer above 100 km is most likely the Na+ within the sporadic E layer in lower E region. However, based upon the well-established Na chemical model, such the neutralization process would be highly difficult because of the low atmospheric density and pressure above 100 km, leaving the formation of such high altitude sporadic Na layer still a mystery. In this paper, we are utilizing and running the classical mesospheric Na chemical model within a sporadic E layer occurring in the lower E region with its background temperature, atmospheric density and pressure modulated by a medium frequency gravity wave to investigate their roles in the formation of the high altitude sporadic Na layer.

### MLTS-03 Height and time characteristics of seasonal and diurnal variations in PMWE based on 1 year observations by the PANSY radar (69.0°S, 39.6°E) by Takanori Nishiyama

Status of First Author: Non-student, PhD

Authors: Takanori Nishiyama, Kaoru Sato, Takuji Nakamura, Masaki Tsutsumi, Toru Sato, Masashi Kohma, Koji Nishimura, Yoshihiro Tomikawa, Mitsumu K. Ejiri, and Takuo T. Tsuda

**Abstract**: We report height and time variations in polar mesosphere winter echoes (PMWE) based on the Program of the Antarctic Syowa mesosphere-stratosphere-troposphere/incoherent scatter (PANSY) radar observations. PMWE were identified for 110 days from March to September 2013. PMWE occurrence frequency increased abruptly in May when two solar proton events occurred. PMWE were also observed even during periods without any solar proton events, suggesting that a possible cause of the PMWE is ionization by energetic electron precipitations. The monthly mean PMWE characteristics showed that occurrence of PMWE were mainly restricted to sunlit time. This fact indicates that electrons detached from negatively charged particles play an important role. While PMWE below 72 km in altitude completely disappeared before sunset, it was detected above that altitude for a few hours even after sunset. This height dependence in the altitude range of 60–80 km can be explained qualitatively by empirical effective recombination rates.

# MLTS-04 The Equatorial OH Airglow Analysis by ISUAL Instrument on Board the FORMOSAT 2 Satellite - by Yi Chung Chiu

Status of First Author: Student IN poster competition, Masters

Authors: Yi Chung Chiu, Loren Chang, J.B Nee

**Abstract**: Airglow is a phenomenon caused by chemical reactions in the mesosphere and thermosphere, which emit visible light at specific wavelengths. Airglow can act as a tracer for certain chemical species, and can be used to infer temperature and wind velocity. As preparation for long term ground-based airglow observations in Taiwan, OH airglow near the mesopause (630 nm wavelength) observed by the ISUAL (Imager of the Sprites and Upper Atmospheric Lightning) instrument on board FORMOSAT 2 is analyzed. The satellite is sun-synchronous and ISUAL CCD camera is limb view scan, so we can use these properties to study the vertical structure of the upper atmosphere in detail. In order to avoid noise from sunlight, the scanning region must avoid the summer hemisphere. Due to this reason, the observations in the middle and low latitudes are much better than the regions approaching the pole. OH airglow is at about from 80~90 km altitude, so we can study the phenomenon in mesosphere and lower thermosphere (MLT) region via OH airglow research. In this report, I choose the images in 2007 of 630 nm filter channel on ISUAL CCD camera to discuss the variation of OH airglow in the low latitude region.

#### MLTS-05 Coordinated temperature measurements in Logan, UT, USA - by Neal R. Criddle

Status of First Author: Student IN poster competition, PhD

Authors: Neal R. Criddle, Tao Yuan, Vincent B. Wickwar, M. J. Taylor, Leda Sox, P.-D. Pautet, Y. Zhao

**Abstract**: In the mesosphere and lower thermosphere (MLT) temperature is an important parameter for the majority of dynamical and chemical processes. Utah State University (USU) in Logan, UT (41.7° N, 111.8° W) and the surrounding area hosts multiple instruments capable of measuring temperatures within the MLT. The USU sodium resonance Doppler lidar measures high resolution 24-hour density, temperature, and wind within the mesopause region (80-110 km). A co-located Rayleigh lidar, assisted by a large poweraperture product provided by a powerful 42 W transmitter and large 4.9 m<sup>2</sup> aperture receiver, measures nightly profiles of relative atmospheric densities and absolute temperatures from 70km up to 115km altitude. An Advanced Mesospheric Temperature Mapper (AMTM) located nearby measures horizontal temperature structure in the OH airglow layer. This study presents an initial comparison between USU's sodium resonance Doppler lidar, Rayleigh lidar, and AMTM temperature observations.

### MLTS-06 Seasonal Variations of TIMED/SABER Carbon Dioxide based Eddy Diffusion Coefficients in the MLT Region - by Cornelius Csar Jude Salinas

Status of First Author: Student IN poster competition, Undergraduate

Authors: Cornelius C.J. Salinas, Loren Chang, Mao-chang Liang, Jia Yue, James Russel III, Amal Chandran and Benjamin Fong Chao

**Abstract**: This work aims to show the seasonal variations of eddy diffusion coefficient vertical profiles in the MLT region estimated using TIMED/SABER satellite CO2 concentrations. Eddy diffusion is a coefficient used to parameterize unresolved processes that mix heat and chemical constituents caused by gravity wave breaking. CO2 is a major gas species in the atmosphere known to have constant concentrations both vertically and horizontally up to around 80 km. Above 80 km, its concentrations begin to have significant vertical and horizontal gradients thus making it susceptible to dynamical transport. It is not very susceptible to photochemical reactions because of its very inert nature. Furthermore, it is very well-known that the variations of CO2 above 80 km are dominantly influenced by gravity wave breaking. Thus, it is an ideal species to use in estimating eddy diffusion coefficients. The eddy diffusion coefficients

are estimated by fitting observed CO2 concentrations from the TIMED/SABER satellite with modelled CO2 concentrations from the 1D JPL/CalTech Model. The eddy diffusion coefficients are assumed to be the reason behind the discrepancies behind observed CO2 and modelled CO2. Thus, we note the adjustments made on the nominal eddy diffusion coefficient profile and determine the possible mechanisms corresponding to these adjustments.

### MLTS-07 Mesospheric winds estimation algorithms for Jicamarca All-Sky Meteor radars by Julio Alberto Oscanoa

Status of First Author: Student NOT in poster competition, Undergraduate

Authors: Julio Oscanoa, Danny Scipión, and Marco Milla

**Abstract**: The Jicamarca All-sky Specular METeor (JASMET) radars are used for detection of specular meteors in the mesosphere and termosphere (70 - 110 km), which in turn are used to estimate the zonal and meridional components of the wind at those ranges.

Open source libraries in the Signal Chain environment were implemented to process the data obtained with the JASMET systems. First, a meteor detection algorithm was developed and a number of filters were used to keep the appropriate underdense meteor echoes, rejecting the inaccurate ones. The selected meteor echoes were grouped to produce wind estimates.

### MLT Other Tidal, PWs, or SSWs

### MLTT-01 Observations of thermosphere and ionosphere changes due to the dissipative 6.5day wave in the lower thermosphere - by Quan Gan

Status of First Author: Non-student, PhD

Authors: Quan Gan, Jia Yue, Loren C. Chang, Wenbin Wang, Shaodong Zhang, Jian Du

**Abstract**: In the current work, temperature and wind data from the Thermosphere Ionosphere Mesosphere Energetics and Dynamics (TIMED) satellite during year 2002-2007 were used to describe the seasonal variations of the westward propagating 6.5-day planetary wave in the mesosphere and lower thermosphere (MLT). Thermospheric composition data from the TIMED satellite and ionospheric total electron content (TEC) from the International Global Navigation Satellite System (GNSS) Service were then employed to carry out two case studies of the effect of this wave on the thermosphere/ionosphere. In both cases, there were westward anomalies of ~ 30-40 m/s in zonal wind in the MLT region that were caused by momentum deposition of the 6.5-day wave, which had peak activity during equinoxes. The westward zonal wind anomalies led to additional poleward meridional flows in both hemispheres. Meanwhile, there were evident overall reductions of thermospheric column density O/N2 ratio and ionospheric TEC with magnitudes up to 16-24 % during these two strong 6.5-day wave events. Based on the temporal correlation between O/N2 and TEC reductions and the extra poleward meridional circulations associated with the 6.5-day waves, we conclude that the dissipative 6.5-day wave (QTDW) as predicted by Yue and Wang [2014].

### MLTT-02 First climatology of temperature structure from 0 to 110 km during 2011-2014 and mechanism study of winter temperature tides of fast amplitude growth above 100 km at McMurdo (77.8S, 166.7E), Antarctica - by Weichun Fong

Status of First Author: Student IN poster competition, PhD

Authors: Weichun Fong, Xinzhao Chu, Xian Lu, Zhibin Yu, Brendan Roberts, Cao Chen, Jian Zhao, Ian Barry, Wentao Huang, Zhangjun Wang, Tim Fuller-Rowell, Arthur D. Richmond, Mihail Codrescu, Chester S. Gardner

**Abstract**: Long-term and year round temperature measurements at high-southern latitudes are rare. Over 5000 hours of lidar data have been collected after the accomplishment of the installation of an Fe Boltzmann lidar system at McMurdo (77.8°S, 166.7°E), Antarctica since late 2010. We established the first temperature climatology based on lidar and radiosonde observations from 2011 to 2014 between 0 and 110 km. We compare the seasonal variation of temperature climatology with other stations in Antarctica such as South Pole (90°S) and Syowa (69°S), such as annual and semiannual variations, mesopause temperature height, and stratopause temperature and height, and etc. Also, McMurdo lidar demonstrates the capability to derive winter temperature from 110 to 120 km, where almost no instrument can provide reliable range-resolved measurements in this region.

The first characterization of diurnal and semidiurnal thermal tides in temperature from 30 to 110 km in the winter season (May through August) at McMurdo reveals that tidal amplitudes grow fast with altitude above 100 km and can reach at least 15 K near 110 km, which are exceeding that of the freely propagating tides originating from the lower atmosphere. Such fast growth exists for all Kp index cases and diurnal amplitude increases to 15–30 K at 110 km with larger Kp indices corresponding to larger tidal amplitudes and faster growth rates. Simulations with the Coupled Thermosphere Ionosphere Plasmasphere Electrodynamics (CTIPe) model reproduce the lidar observations and exhibit concentric ring structures of diurnal amplitudes encircling the south geomagnetic pole and overlapping the auroral zone. These findings point to a magnetospheric source origin. Mechanistic studies using CTIPe show that the adiabatic cooling/heating associated with Hall ion drag is the dominant source of this feature, while Joule heating is a minor contributor due to the counteraction by Joule-heating-induced adiabatic cooling. The sum of total dynamical effects and Joule heating explains ~80% of the diurnal amplitudes. Auroral particle heating, lower atmosphere tides, and direct solar heating have minor contributions.

### MLTT-03 Seasonal and quasi-biennial variations in ionospheric tidal signatures using HHT analysis - by Loren Chang

Status of First Author: Non-student, PhD

#### Authors: Loren C. Chang, Yan-Yi Sun, Jack Wang, Shih-Han Chien

**Abstract**: Tidal analysis is a convenient method for isolating global scale spatial and local time features of the ionosphere, both excited in-situ, as well as through coupling with the middle and lower atmosphere. In this study, we examine the coherent spatial and temporal modes dominating the variation of selected ionospheric tidal and stationary planetary wave signatures from FORMOSAT-3/COSMIC observations using Hilbert-Huang Transform (HHT) analysis. In particular, we examine the DW1 migrating diurnal component, previously associated with in-situ photoionizaton; as well as the DE3 and SPW4 components, which are driven by lower atmospheric sources and form the wave-4 EIA signature. HHT analysis is found to be effective at resolving the seasonal and solar cycle variation of these components, while also resolving an equatorial quasi-biennial variation in all three cases. The possible relation of this quasi-biennial variation with the middle atmosphere quasi-biennial osccillation (QBO) manifested in SABER tidal observations, as well as similar periodicities in solar and geomagnetic parameters is discussed.

### MLTT-04 A Study of thermospheric-ionospheric response to the 2009 stratospheric sudden warming by using an assimilative TIME-GCM with SAMI3 model simulations by Jia-Ting Lin

Status of First Author: Student IN poster competition, PhD

Authors: J. T. Lin, C. H. Lin, L. C. Chang, H.-L. Liu, Y. T. Chen, J. D. Huba and J. Y. Liu

**Abstract**: In this study, we investigate the responses of tidal winds and neutral compositions in thermosphere to the 2009 stratospheric sudden warming (SSW) and examine their impacts on ionospheric perturbations. The TIME-GCM has assimilated MERRA meteorological reanalysis data between the

lower-boundary (~30km) and 0.1h Pa (~62km) by a nudging method rather than imposed as an external forcing at the lower boundary. Taking advantage of vertical range of forcing, we were able to study the coupling more realistically in this warming episode, the simulation successes to represent the typical SSW ionospheric effect (morning enhancement/afternoon reduction in TEC). Therefore, significant change are found in the migrating semi-diurnal tides (SW2) in the E-region during SSW period, the amplitudes of SW2 shows a pronounced reduction/enhancement at middle to high latitude during/after the SSW as well as with the earlier phase shift at constant altitude, it is resulting from the shortening of vertical wavelength due to reversal mean wind condition in mesosphere. The amplitude and phase variability of the SW2 at middle to high latitude is found to be capable of producing significantly temporal variability in the vertical plasma drift in equatorial region. The influence of tidal mixing effect in the thermosphere on reducing O/N2 ratio is also investigated, it caused an overall decrease of electron density in low-latitude ionosphere during SSW period. Further, these thermospheric responses (wind/compositions) to the 2009 SSW from the TIME-GCM were individual or together to drive the one-way coupling SAMI3 model, comparing the changes of vertical plasma drift and TEC to discuss the importance of occurring in the ionosphere response to SSW.

### MLTT-05 Lidar and satellite studies of the vertical coupling of eastward propagating planetary waves with periods of 1–5 days from the stratosphere to the lower thermosphere in the winter Antarctic - by Xian Lu

Status of First Author: Non-student, PhD

Authors: Xian Lu, Xinzhao Chu, Cao Chen, Vu Nguyen

Abstract: Following the work by Lu et al. [2013] which has shown that the stratospheric temperature variations are largely determined by a group of eastward propagating planetary waves (PWs) relative to ground with periods of 1-5 days, the impacts of the same group of PWs are identified in the mesosphere and lower thermosphere (MLT) region (80–110 km), using the nearly continuous temperature measurements for 6 days by the Fe lidar at McMurdo, Antarctica (77.8°S, 166.7°E) and by the MLS onboard the Aura satellite. The Fe lidar observations show dominant peaks at 5 day and its sub-harmonics. The wave amplitudes decrease above the source region of 40-50 km, while gradually increase above 80 km and reach a maximum of 10 K near 110 km. The nearly continuous phase progressions with altitude imply a direct propagation of waves from the lower to the upper atmosphere, from which the vertical wavelengths are estimated to be ~70 km. These features imply that although the PWs experience significant dissipation as they propagate away from the strong polar vortex and upward to the mesosphere, they can still penetrate to and have non-negligible impacts in the lower thermosphere. The reconstruction field at McMurdo from the global MLS temperature measurements captures the main patterns of temperature fields induced by PWs and the dominant wavenumbers are characterized. This is the first time to identify the PW influences in the lidar temperatures observed in the polar MLT region, and with considerable magnitudes. It is also the first time that the global satellite data are used to interpret the local temperature variability at McMurdo that are caused by the different components of eastward propagating PWs generated by the instability of the polar vortex in the stratosphere.

### MLTT-06 Interhemispheric Comparison of Seasonal Mesospheric Tidal Activity observed by mid-latitude SuperDARN Radars - by Garima Malhotra

Status of First Author: Student IN poster competition, Masters

Authors: Garima Malhotra, J. Michael Ruohoniemi, Joseph B. H. Baker

**Abstract**: Meteor wind measurements obtained by mid-latitude SuperDARN radars are used to study mesospheric tidal behaviour in the Northern and Southern Hemisphere from 2010-2013. Our analysis technique builds upon previous work by Hall et al. [1997] in that it employs refined methods to extract meteor scatter from "Grainy Near Range Echoes" and differentiate them from other sources, such as sporadic E-layer and ground scatter. The results are compared with measurements obtained by radars at higher latitudes and the HWM07 model averaged over an altitude range of 85-95 km. We find the tidal

amplitudes in the Southern Hemisphere are significantly greater than the amplitudes in the Northern Hemisphere and there are significant differences in seasonal behaviour of the semidiurnal and diurnal tides between the hemispheres. We also see notable model-data inconsistencies such that the model tends to overestimate the zonal and meridional components in both hemispheres. We discuss the various influences that may be responsible for producing these differences.

### MLTT-07 Seasonal variations of MLT tides revealed by a meteor radar chain based on HMD analysis - by You Yu

Status of First Author: Non-student, PhD

Authors: You Yu and Weixing Wan

Abstract: Seasonal variations of different tides in the mesosphere and lower thermosphere are investigated from a meteor radar chain on the basis of Hough mode decomposition. More than 4 years wind observations are collected from the meteor radar chain. Firstly, the observed winds are decomposed into different (diurnal, semidiurnal and terdiurnal) tidal components. Different seasonal patterns are revealed for each component. Pronounced semiannual oscillation (SAO) is presented in the diurnal component. While latitude-depended seasonal variation is found in the semidiurnal and terdiurnal components. At the low/mid- latitude stations, the semiannual/annual oscillation is relatively stronger. Then, Hough mode decomposition is utilized to extract the dominant tidal modes of each decomposed component. It is found that each component is dominated by one of its symmetric tidal modes with strong seasonal dependency. Apparent SAO is observed in the dominant (1, 1) mode; (2, 4) mode is strong after Sep. equinox and around Dec. solstice. Based on the extracted results we further map the three-dimensional distribution (latitude x altitude x season) of each tidal component. The mapped results are finally compared with the corresponding values observed by the Thermosphere Ionosphere Mesosphere Energetics and Dynamics (TIMED) Doppler Interferometer (TIDI) and modeled from the Global Scale Wave Model (GSWM). Each mapped tidal component agrees well with corresponding TIDI observation in the seasonal variation. Meanwhile, coincidences are found in the seasonal dependency of the diurnal component between the mapped values and the modeled results from GSWM, while difference between them exists in that of the semidiurnal one.

### MLTT-08 Observations of Secondary Waves Arising from QTDW-DW1 Interaction by Vu Nguyen

Status of First Author: Student IN poster competition, PhD

Authors: Ruth Lieberman and Scott Palo

**Abstract**: Theory and past observations have provided evidence that atmospheric tides and other global scale waves may nonlinearly interact to produce additional secondary waves throughout the spaceatmosphere interaction region. However, very few studies have investigated the generation region of nonlinearly secondary waves and as a result, the manifestation and impacts of these waves are still poorly understood. This study focuses on the nonlinearly interaction between the quasi two-day wave and the migrating diurnal tide, two of the largest global scale waves in the atmosphere. The main goal of this study is to characterize the forcing region of the secondary waves and understand how it relates to their manifestation on a global scale. Techniques are first applied to Aura-MLS and TIMED-SABER satellite observations of temperatures to estimate the amplitude and phase of the quasi-two day wave (QTDW), migrating diurnal tide (DW1) and secondary waves within short temporal windows. Estimates of the QTDW and DW1 in the zonal and meridional wind fields are also derived from observations. By utilizing the primary wave estimates in the horizontal wind and temperature fields, the momentum and thermal forcing region of the secondary waves arising from a QTDW-DW1 interaction are assessed over multiple years for the first time.

### MLTT-09 Stationary planetary waves and their momentum budgets in eCMAM30 - by Mary Beth Bradley

Status of First Author: Non-student, PhD

Authors: Beth Bradley, Quan Gan, Jian Du, William Ward

**Abstract**: In recent years, much attention has been given to stationary planetary waves (SPWs) appearing in the mesopause region (approximately 100 km height), expecially in the winter hemisphere. These SPWs signatures near the mesopause show different seasonal variations from those in the stratosphere. They are present throughout the year, even in the summer hemisphere, and extend into the tropics. Many questions remain unanswered concerning the generation of these waves, particularly in the tropics and the summer hemisphere: What sources contribute to the generation of these waves? Are they derived from waves generated in the troposphere or stratosphere that have propagated upward or is there another source, which originates in the mesospause region?

In this project, we employ data from the eCMAM30 run (the extended Canadian Middle Atmosphere Model, extending from the Earth's surface to ~220 km). The eCMAM30 is nudged toward ERA-Interim – the European Centre for Medium-Range Weather Forecasts (ECMWF) reanalysis data – up to the pressure level of 1 hPa for the period of 1979–2010. The SPWs (wavenumbers 1 to 5) from eCMAM30 show very good agreement with SABER observations from 20 to 110 km. We examine the momentum budget terms of SPWs (e.g. coriolis force, pressure gradient force, linear and non-linear advection, gravity wave drag, etc.) in eCMAM30 for indications of potential sources for these waves.

### MLTT-10 Photochemical modeling of nonmigrating tides in the 15 µm infrared cooling of the lower thermosphere and comparison with SABER - by Nirmal Nischal

Status of First Author: Student IN poster competition, Masters

Authors: Nirmal Nischal, Jens Oberheide, Martin G. Mlynczak, Linda A. Hunt, Astrid Maute

**Abstract**: Our earlier tidal diagnostics of SABER CO2 15 µm data showed a substantial modulation of the energy budget of the lower thermosphere due to nonmigrating tides: relative amplitudes of the CO2 cooling rates for the DE2 and DE3 components were on the order of 15-50% with respect to the monthly mean emissions. We now perform a photochemical tidal modeling using TIME-GCM background and tides from the empirical CTMT model. Although there are systematic amplitude differences, general amplitude structures are well reproduced and phases compare favorably to the observation. Furthermore, we isolate the relative contributions of temperature, density and advection in order to understand the underlying coupling mechanisms responsible for transmitting the tidal signal into the CO2 cooling rates. While the main tidal coupling mechanism is the temperature dependence of the collisional excitation of the CO2 (01101) fundamental band transition (v2), the response to neutral density variations is also important. Neutral density becomes as important as temperature above 115 km as such explaining an unexpected tidal phase behavior in the observation. However, the contribution of vertical advection is comparatively small. A sensitivity analysis indicates that the current uncertainties in the background temperature and atomic oxygen used for the photochemical modeling do not impact our conclusion about the relative importance of temperature, neutral density and vertical advection.

### MLTT-11 Statistical characteristics of short-term variability of diurnal tides in eCMAM30 - by Ashan Vitharana

Status of First Author: Student IN poster competition, Masters

Authors: Jian Du :Department of Physics and Astronomy, University of Louisville, Louisville, KY Jens Oberheide :Department of Physics, Clemson University, Clemson, SC

**Abstract**: In this research we investigate statistical characteristics of the short-term variability (on the order of 4 days) of the diurnal tides and illustrate how these statistical characteristics change with season, latitude and altitude from the troposphere to the thermosphere/ionosphere, using data from the extended Canadian Middle Atmosphere Model (eCMAM30) run (1979-2010). In this approach statistical frequency probability density functions (PDFs) were developed to examine the underlying statistics governing the short-term tidal variability and to what extent these PDFs changes temporally and spatially. Four moments associated with the PDF were examined, namely, the mean, variance, skewness, and kurtosis (or flatness) as a function of altitude, latitude and time. Wavelet analysis is also used to analyze localized variations of power within the time series.

### MLTT-12 Seasonal variations of Hough modes in DW1 and DS0 - by David Warder

Status of First Author: Student IN poster competition, Masters

Authors: David M. Warder, Jian Du, Dave Mackenzie, William E. Ward

**Abstract**: In 1898, S.S. Hough developed a set of solutions to Laplace's tidal equations that provided a complete basis set for describing ocean tides; later adapted to atmospheric tides. Hough mode decomposition allows an analysis of the latitudinal, altitudinal, and temporal structure of tidal waves. We apply this methodology to decompose the DW1 and DS0 tides in the Extended Canadian Middle Atmospheric Model (eCMAM) in order to compare and contrast the symmetries in seasonal variation exhibited by these two tides. These two tidal components are particularly interesting since DS0 exhibits a seasonally symmetric variation with both hemispheres strengthening simultaneously, whereas DW1 strengthens asymmetrically so that when one hemisphere is strong, the other is weak.

### MLTT-13 Influence of the sudden stratosphere warming on quasi-2 day waves by Shengyang Gu

Status of First Author: Student NOT in poster competition, PhD

#### Authors: Shengyang Gu, Hanli Liu, Tao Li, Xiankang Dou

**Abstract**: The influence of the sudden stratosphere warming (SSW) on quasi-2 day wave (QTDW) with westward zonal wavenumber 3 (W3) are investigated using the Thermosphere-Ionosphere-Mesosphere-Electrodynamics General Circulation Model (TIME-GCM). The summer easterly jet below 90 km is strengthened during an SSW, which results in a larger refractive index and thus more favorable condition for the propagation of W3. In the winter hemisphere, the Eliassen Palm (EP) flux diagnostics indicate that the strong instabilities at middle and high latitudes in the mesopause region are important for the amplification of W3, which are weakened during SSW periods due to the deceleration or even reversal of the winter westerly winds. Nonlinear interactions between the W3 and the wavenumber 1 stationary planetary wave produce QTDW with westward zonal wavenumber 2 (W2). The meridional wind perturbations of the W2 peak in the equatorial region, while the zonal wind and temperature components maximize at middle latitudes. The EP flux diagnostics indicate that the W2 is capable of propagating upward in both winter and summer hemispheres, whereas W3 is able to propagate in the summer hemisphere. This characteristic is likely due to the fact that the phase speed of W2 is larger, and therefore its waveguide has a broader latitudinal extension. The larger phase speed also makes W2 less vulnerable to dissipation and critical layer filtering by the background wind when propagating upward.

# MLTT-14 Examination of sudden stratospheric warming effects of non-migrating diurnal tides - by Austin Gornet

Status of First Author: Student IN poster competition, Undergraduate

Authors: Austin D Gornet and Jian Du

**Abstract**: Non-linear interactions between so called "parent wave" the stationary planetary waves (SPW1 or SPW2) and migrating diurnal tide (DW1) to produce "child waves" nonmigrating diurnal tides (DS0/DW2 or DE1/DW3) have been rigorously theorized. Here we seek to examine their effects on the nonmigrating diurnal tides during a sudden stratospheric warming (SSW) event with known amplified SPWs. For this study, we use the 2003-04 winter SSW event in the eCMAM30 (the extended Canadian Middle Atmosphere Model, 1979-2010) run data analogous to a similar examination performed by Pancheva et al. (2009) with SABER/TIMED data. We specifically examine the amplification or diminution of the SPW1, SPW2, DS0, DE1, DW1, DW2, DW3 tides below 120 km as well as their spatial structure and evolution for evidence of the SPWs/tidal interactions. This is a first step in a project that will examine every warming event within the eCMAM30 run to expose the SPWs/tidal nonlinear interactions of most import for minor, split, and displacement warming events.

# MLTT-15 Neutral Temperature and Horizontal Wind in the Thermosphere – by Brittany A. Marriott

Status of First Author: Student IN poster competition, Undergraduate

#### Authors: Brittany Marriott and Titus Yuan

**Abstract**: Neutral temperature and horizontal wind measurements in the thermosphere are difficult to achieve, whereas they are critical parameters for all kinds of chemical and dynamic processes. The ion temperature and velocity are believed to be the close proxies for natural temperature and wind in the lower thermosphere, where the ion-neutral collision rate is high. In this paper, we combine the monthly climatology from the Millstone Hill Incoherent Scatter Radar (ISR) with that derived from the multi-year full diurnal cycle Na lidar data to achieve a hybrid climatology that covers the altitude range from 80 km to 150 km. We also derive the tidal wave perturbations in the lower thermosphere (100 km - 120 km), from the hypothetical scenario in which an Na Doppler/temperature lidar is running alongside an ISR, to show the potential of measuring critical tidal information within the turbo-pause region by the simultaneous observations from the two instruments.

### **Sprites**

# SPRT-01 Analysis of two thunderstorms producing three negative sprites on 12 September 2014 - by Levi Boggs

Status of First Author: Student IN poster competition, Masters

Authors: Levi Boggs, Ningyu Liu, Michael Splitt, Steven Lazarus, Steven Cummer

**Abstract**: Powerful cloud-to-ground (CG) lightning in thunderstorms can produce strong quasielectrostatic fields in the upper atmosphere causing brief, luminous electrical discharges in the lower ionosphere, which are known as sprites. These upper atmospheric electrical phenomena are driven by tropospheric lightning and rely on CG strokes to remove large amounts of thunderstorm charge in a very short amount of time. Sprites can be either of negative or positive polarity which is determined by the polarity of the parent CG discharge. Negative sprites are extremely rare when compared to their positive counterparts and the thunderstorms that produce negative sprites differ dynamically and electrically from positive sprite producing thunderstorms [Lang et al., JGR, 115, A00E22, 2010; Lang et al., JGR, 118, 2013].

Typically for negative sprites to be triggered, more charge must be removed from the thundercloud in a shorter period of time when compared to positive sprites, thus requiring a more impulsive parent lightning stroke. It has been found that negative sprite parent CG lightning primarily consists of bolt-from-the-blue (BFB) and hybrid intra-cloud negative cloud-to-ground (IC-NCG) lightning [Lang et al., JGR, 116, A10306, 2011; Lu et al., JGR, 117, D04212, 2012]

Here we present a detailed analysis of three negative sprite events that were captured by a low-light-level camera on 12 September 2014. The events occurred above two storms in central and south Florida. We will present the data collected by several lightning location networks and dual-polarization weather radar. We will discuss the detailed development of the parent CGs and attempt to explain why they are particularly effective in quickly removing charge from thunderstorms to ground so as to generate the observed negative sprites.

### SPRT-02 Effects of Thunderstorm Electrostatic Fields on the Conductivity of the Lower Ionosphere - by Mohammad Ahmad Salem

Status of First Author: Student IN poster competition, PhD

Authors: Mohammad A. Salem, Ningyu Liu, and Hamid K. Rassoul

**Abstract**: The conductivity of the lower ionosphere plays an important role in the propagation of very low frequency (VLF) waves in the Earth-ionosphere waveguide. It can be affected by thunderstorm electric fields through the interplay between two field-dependent quantities: the ionospheric electron density and the electron mobility, which manifests itself as the heating effect.

Recently, we have demonstrated that small electrostatic fields, of values not strong enough to produce transient luminous events (TLEs), can be established in the lower ionosphere due to underlying thunderstorms. Using a simplified ion chemistry model described by Liu [J. Geophys. Res., 117, A03308, 2012], we have found that under steady state conditions, the nighttime electron density profile can be reduced by up to ~40% or enhanced by a factor of up to ~6 because of the variation of the three-body electron attachment rate constant with the electric field [Salem et al., Geophys. Res. Lett., 42(6), doi: 10.1002/2015GL063268, 2015]. In this talk, we investigate the modification of the conductivity of the lower ionosphere by taking into account both of the changes in the electron density and mobility due to the thunderstorm electrostatic field.

We have modified our model in order to self-consistently calculate the steady-state ionospheric conductivity above a thunderstorm. The results from this new model indicate that the conductivity can be modified significantly. Finally, we will compare the results with a recent measurement that show thunderstorms can reduce the ionospheric conductivity by several orders of magnitude on a longer time scale [Shao et al., Nat. Geosci., doi: 10.1038/NGEO1668, 2012].

### SPRT-03 Preliminary Results of a Software Defined Radar System to Detect Sprites by Salih Mehmed Bostan

Status of First Author: Student NOT in poster competition, PhD

Authors: Salih M. Bostan, Julio V. Urbina, John D. Mathews

**Abstract**: Lightning triggered transient luminous events (TLEs) are optical phenomenons that occupy large volumes in the upper-atmosphere and D-region of the ionosphere. Sprites are TLEs that mostly occur at 55 km to 95 km altitude and perturb several hundred electrons per cc with lifetimes of order of a second. In this poster, preliminary results and details of a software defined radar system to detect sprites are given. The system is deployed at Rock Springs, PA in order to test it's functionality, however the actual experiment is expected to be conducted in a location where percent of thunderstorms is high. The radar system is using two USRP1s in order to generate probing signal and to collect data.

### **Stratosphere Studies and Below**

### STRA-01 Comparing USU Rayleigh Lidar and Assimilative Model Temperatures at 45 km - by David K. Moser

Status of First Author: Student IN poster competition, Masters

#### Authors: David K. Moser, Vincent B. Wickwar, Joshua P. Herron, David L. Barton

**Abstract**: While many atmospheric models provide temperature data up to or above 45 km, supporting observations at such altitudes are unfortunately few and far between. A Rayleigh-scatter lidar system at the Atmospheric Lidar Observatory (ALO-USU; 41.74° N, 111.81° W) has operated since 1993 as part of Utah State University's Center for Atmospheric and Space Sciences (CASS), providing extensive observational data from which absolute temperatures in the middle atmosphere can be derived. Of obvious interest to anyone relying on currently available reanalysis models is how well their upper bounds correspond to these kinds of real observations. Using over 700 nights of ALO-USU Rayleigh-scatter lidar data taken between 1993 and 2004, the following work compares real, all-night, observational temperatures at 45 km with those given by a model from the Climate Prediction Center (CPC), the European Centre for Medium-Range Weather Forecasts' (ECMWF) ERA-Interim model, and NASA's Modern-Era Retrospective Analysis for Research and Applications (MERRA) model. Of particular note are significant outliers, both positive and negative, in the ALO-USU temperatures that correspond to similar outliers in the models. This relationship suggests an origin in lower-altitude meteorological activity that propagates upward.

Agner, Matthew, 14 Barry, Ian, 20 Boggs, Levi, 31 Bossert, Katrina, 20 Bostan, Salih, 32 Bradley, Mary 28 Cai, Xuguang, 23 Cao, Bing, 15 Chang, Loren, 26 Chen, Cao, 21 Chiu, Yi Chung, 24 Criddle, Neal, 24 Dawkins, Erin, 22 de Wit, Rosmarie, 2 Eastes, Richard, 1 Evans, W.F.J., 4 Fletcher, Alex, 13 Fong, Weichun, 25 Gan, Quan, 8, 25 Gao, Boyi, 9 Gasperini, Federico, 1 Gay, Johnathon, 19 Goel, Ashish, 10 Gornet, Austin, 30 Grawe, Matthew, 2 Gu, Shengyang, 30 Guo, Yafang, 21 Haaser, Robert,9 Hall, Stephen, 5 Heale, Christopher, 14 Hew, Yayu Monica, 11 Huang, Wentao, 22 Inonan, Marcos, 5 Johnson, Stuart, 7 Kam, Hosik, 15 Kellett, Daniel, 11

Kim, Jeong-Han, 8 Lay, Erin, 13 Li, Haoyu, 17 Li, Jintai, 6 Limonta, Lorenzo, 11 Lin, Cissi, 2 Lin, Jia-Ting, 26 Lu, Xian, 27 Lucas, Greg, 3 Mabie, Justin, 4 Malhotra, Garima, 27 Marriott, Brittany, 31 McInerney, Joe, 3 Mehta, Dhvanit, 16 Moser, David, 32 Navarro Dominguez, Luis, 8,19 Negale, Michael, 16 Nguyen, Vu, 28 Nischal, Nirmal, 29 Nishiyama, Takanori, 23 Nossa, Eliana, 6 Oscanoa, Julio, 25 Panka, Peter, 6 Pilinski, Marcin, 4 Pugmire, Jonathan, 16 Salem, Mohammad, 32 Salinas, Cornelius Csar Jude, 24 Spangler, Benjamin, 13 Sox, Leda, 21 Talaei, Ahmad, 17 Tarano, Ana, 12 Tarnecki, Liane, 12 Triplett, Colin, 17 Vail, Chris, 17 Vaudrin, Cody, 7 Vitharana, Ashan, 29

Wang, Jack, 4

Warder, David, 30 Wickwar, Vincent, 20

Yu, You, 28

Zhang, Yun, 15 Zhu, Qian, 12